Supporting Information

A unified approach toward the rational design of selective low nanomolar Human Neutrophil Elastase Inhibitors

Laurinda R. P. Areias, Eduardo F. P. Ruivo, Lídia M. Gonçalves, M. Teresa Duarte, Vânia André, Rui Moreira, Susana D. Lucas and Rita C. Guedes

Table of Contents

1 Pharmacophore Modeling

1.1 Pharmacophore Training Set

S1
IC$_{50}$ 44nM

S2
K$_{on}$ 3.24x10^6 M^{-1}s^{-1}

S3
K$_{on}$ 1.77x10^6 M^{-1}s^{-1}

S4
K$_{on}$ 2.28x10^6 M^{-1}s^{-1}

S5
K$_{on}$ 3.18x10^6 M^{-1}s^{-1}

S6
K$_{on}$ 1.17x10^6 M^{-1}s^{-1}

S7
K$_{on}$ 6.47x10^5 M^{-1}s^{-1}

S8
K$_{on}$ 6.61x10^5 M^{-1}s^{-1}

S9
K$_{on}$ 5.08x10^5 M^{-1}s^{-1}

S10
K$_{on}$ 1.66x10^5 M^{-1}s^{-1}

S11
K$_{on}$ 2.86x10^5 M^{-1}s^{-1}

S12
IC$_{50}$ 5 nM

S13
IC$_{50}$ 8.1nM

S14
IC$_{50}$ 22 nM

S15
IC$_{50}$ 29 nM

S16
IC$_{50}$ 39 nM

S17
IC$_{50}$ 57 nM

S18
IC$_{50}$ 61 nM

S19
IC$_{50}$ 65 nM

S20
IC$_{50}$ 93 nM
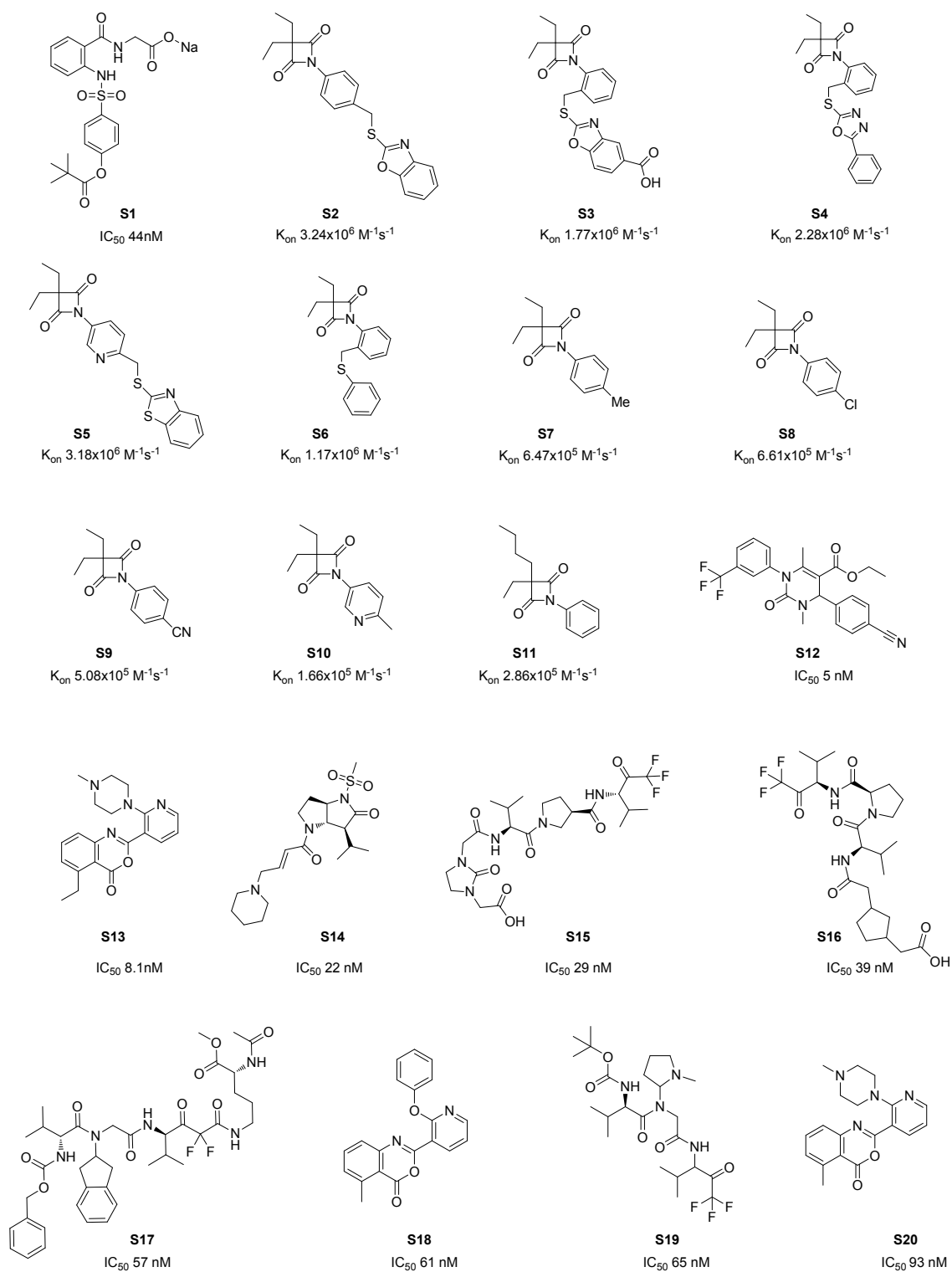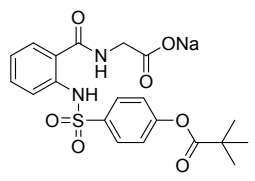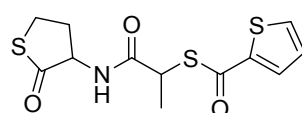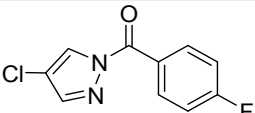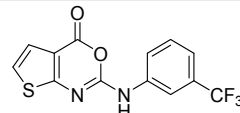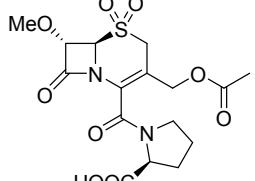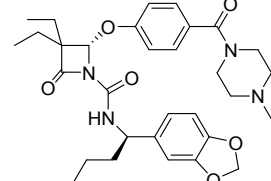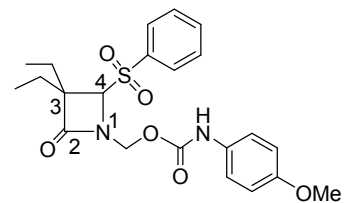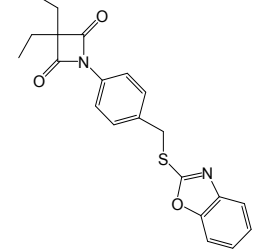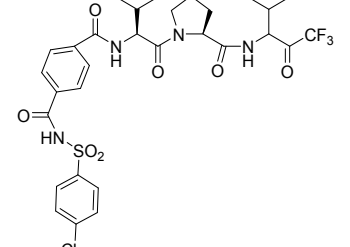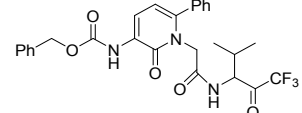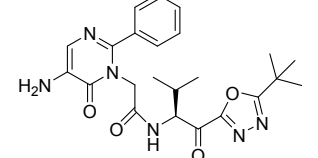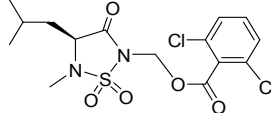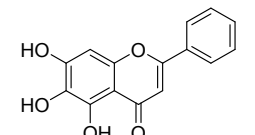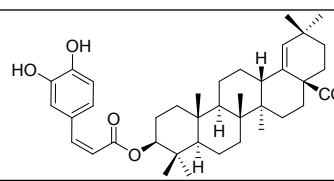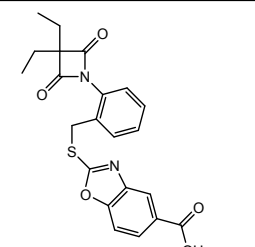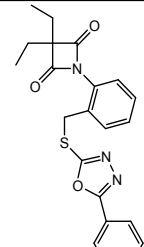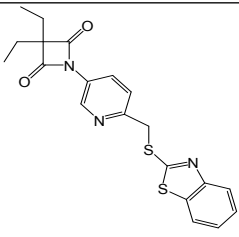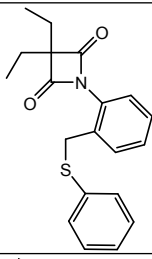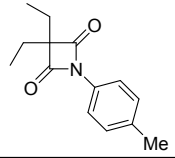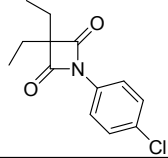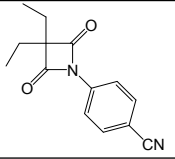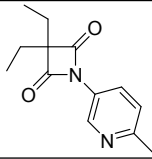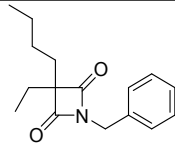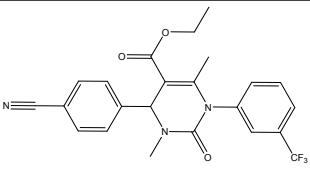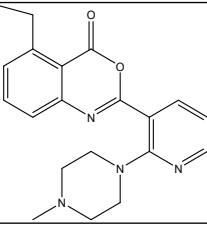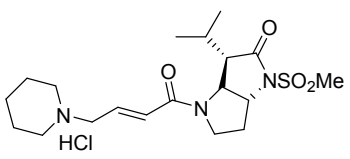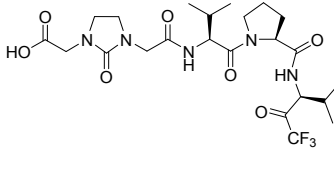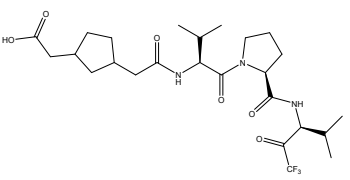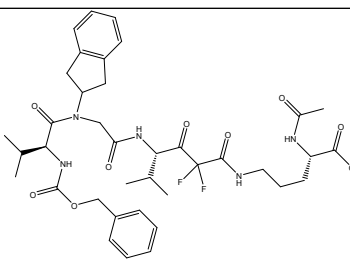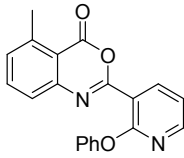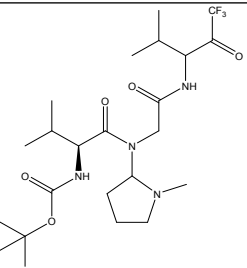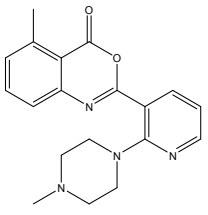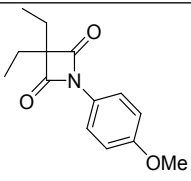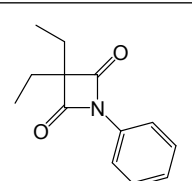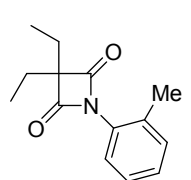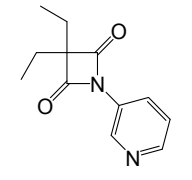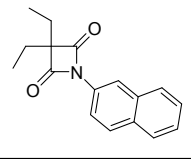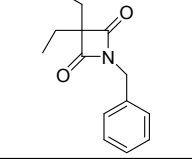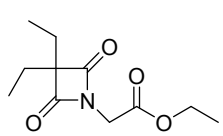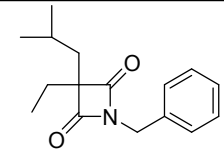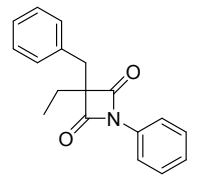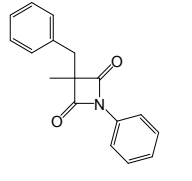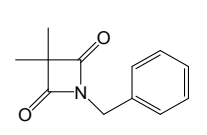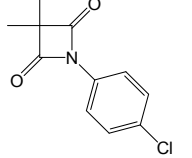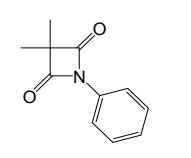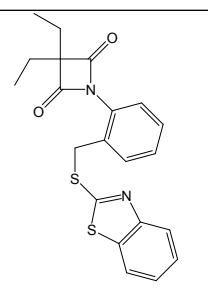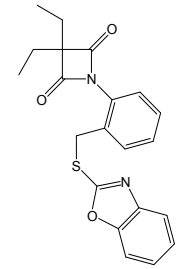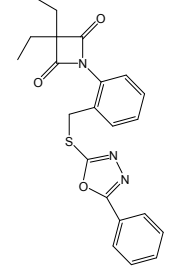
Figure S1. Training Set
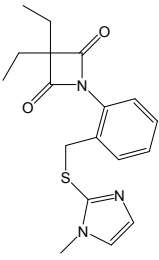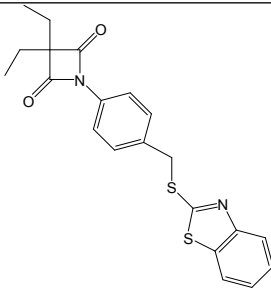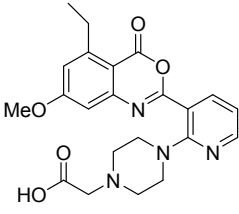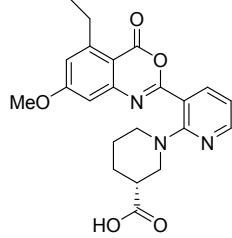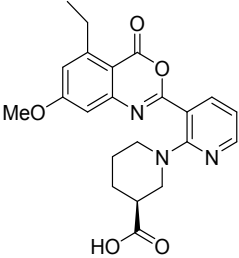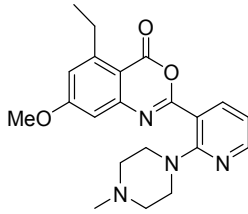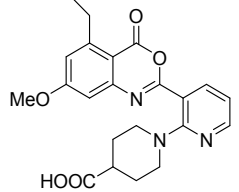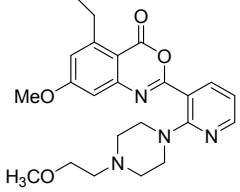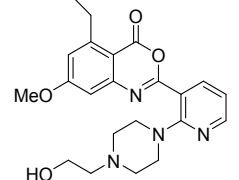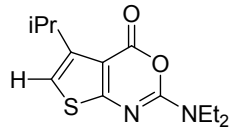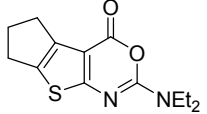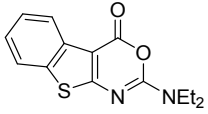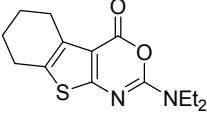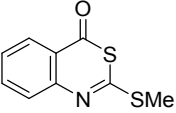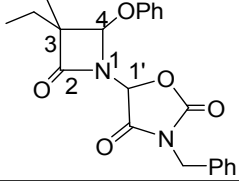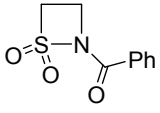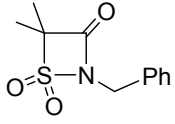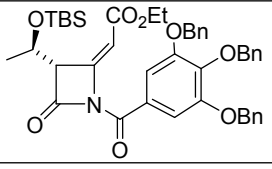
1.2 Pharmacophore Positive Control Test Set
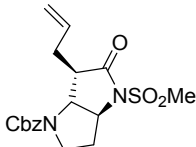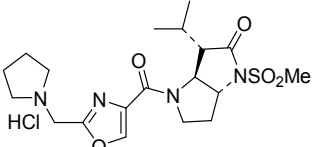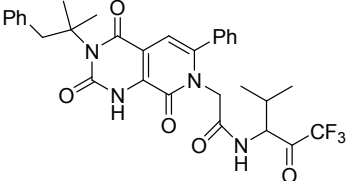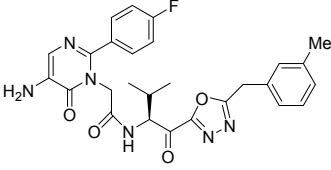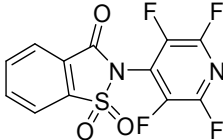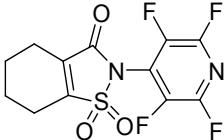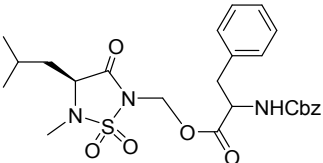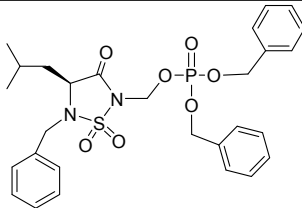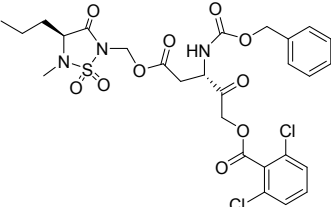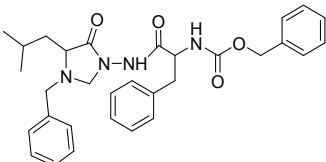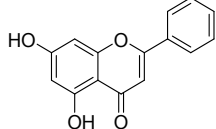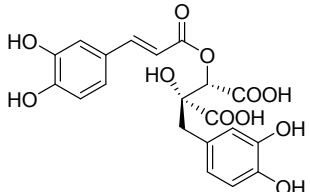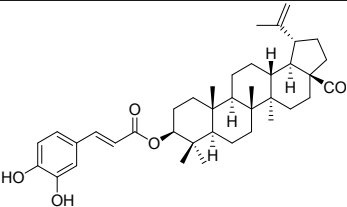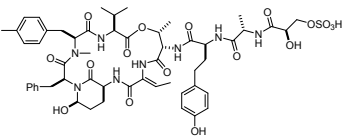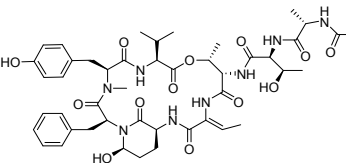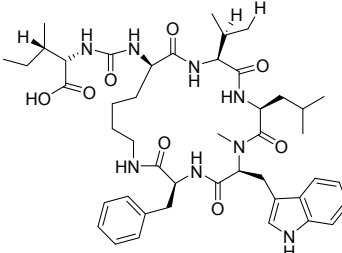
TableS1. Pharmacophore Positive Control Test Set
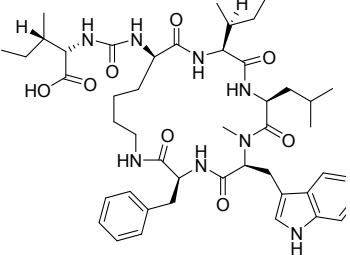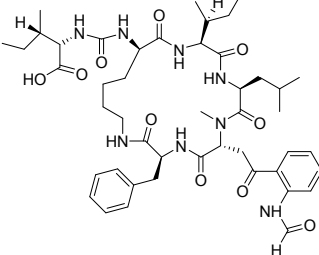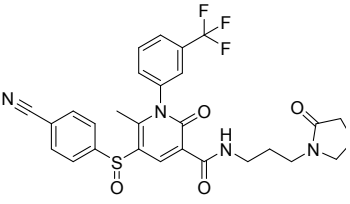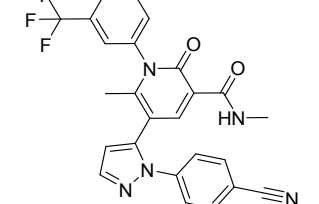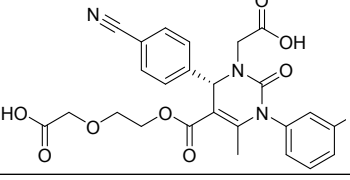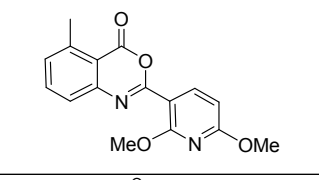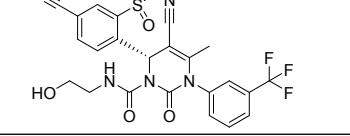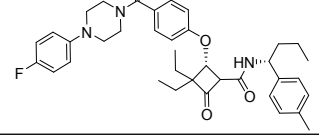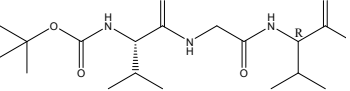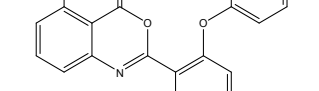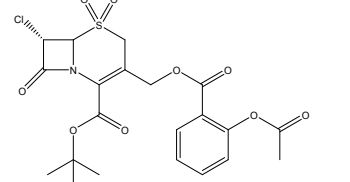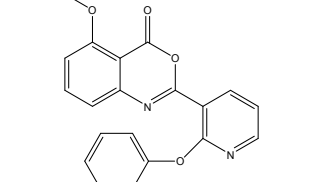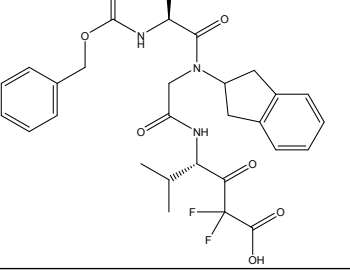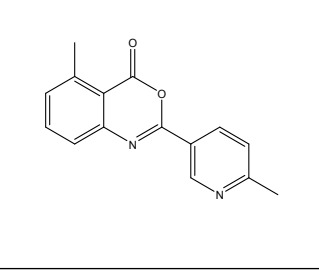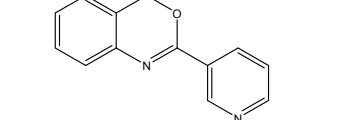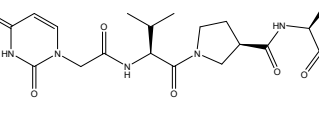
Compound	Activity[ref]	Compound	Activity[ref]
	IC$_{50}$ 44 nM[1]		K_i 1.4 µM[22]
	K_i 6 nM[3]		K_i 4 µM[4]
	k_{obs}/[I] 3800 M^{-1} s^{-1}[5]		k_{on}/[I] 3.8x10^6 M^{-1}s^{-1}[6]
	k_{obs}/[I] 100.3 M^{-1}s^{-1}[7]		k_{on} 3.2x10^6 M^{-1}s^{-1} [8]
	K_i 0.2 nM[9]		K_i 4.5 nM[10]
	K_i 12.1 nM[11]		K_{inact}/k_i 4.9x10^6 M^{-1}s^{-1}[12]
	IC$_{50}$ 2.2 µM[13]		IC$_{50}$ 0.32 µM[14]
	k_{on} 1.77x10^{6}M^{-1}s^{-1}[8]		k_{on} 2.3x10^6 M^{-1}s^{-1}[8]
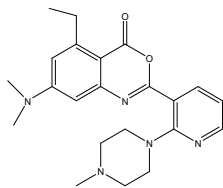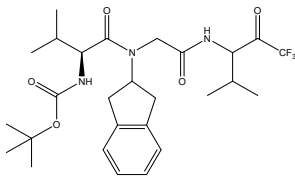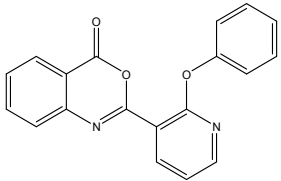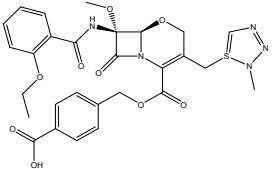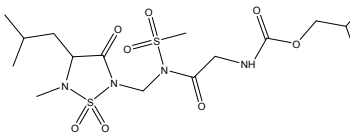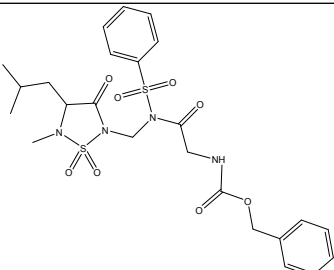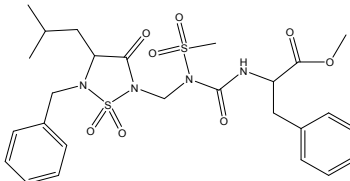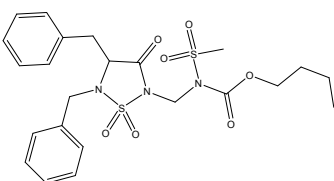
Compound	Activity[ref]	Compound	Activity[ref]
	k_{on} 3.2×10^6 M^{-1}s^{-1}[8]		k_{on} 1.2×10^6 M^{-1}s^{-1}[8]
	k_{on} 6.5×10^5 M^{-1}s^{-1}[8]		k_{on} 6.6×10^5 M^{-1}s^{-1}[8]
	k_{on} 5.1×10^5 M^{-1}s^{-1}[8]		k_{on} 1.7×10^5 M^{-1}s^{-1}[8]
	k_{on} 2.9×10^5 M^{-1}s^{-1}[8]		IC$_{50}$ 5 nM[15]
	IC$_{50}$ 8.1 nM[16]		IC$_{50}$ 0.022 µM[17]
	IC$_{50}$ 29 nM[18]		IC$_{50}$ 39 nM[19]
	IC$_{50}$ 57 nM[20]		IC$_{50}$ 61 nM[21]
	IC$_{50}$ 65 M[22]		IC$_{50}$ 93 nM[21]

Compound	Activity[ref]	Compound	Activity[ref]
	k_{on} 3.1×10^5 M^{-1}s^{-1}[8]		k_{on} 2.4×10^5 M^{-1}s^{-1}[8]
	k_{on} 1.1×10^3 M^{-1}s^{-1}[8]		k_{on} 1.0×10^5 M^{-1}s^{-1}[8]
	k_{on} 4.4×10^3 M^{-1}s^{-1}[8]		k_{on} 1.8×10^3 M^{-1}s^{-1}[8]
	k_{on} 7.3×10^2 M^{-1}s^{-1}[8]		k_{on} 2.9×10^4 M^{-1}s^{-1}[8]
	k_{on} 2.0×10^3 M^{-1}s^{-1}[8]		k_{on} 2.7×10^2 M^{-1}s^{-1}[8]
	k_{on} 6.2×10^3 M^{-1}s^{-1}[8]		k_{on} 3.9×10^5 M^{-1}s^{-1}[8]
	k_{on} 1.9×10^5 M^{-1}s^{-1}[8]		k_{on} 1.5×10^4 M^{-1}s^{-1}[8]
	k_{on} 3.5×10^4 M^{-1}s^{-1}[8]		k_{on} 6.0×10^4 M^{-1}s^{-1}[8]

Compound	Activity[ref]	Compound	Activity[ref]
	k_{on} 1.3×10^3 M^{-1}s^{-1}[8]		k_{on} 1.2×10^6 M^{-1}s^{-1}[8]
MeO	IC$_{50}$ 23 nM[21]	MeO	IC$_{50}$ 19 nM[21]
MeO	IC$_{50}$ 25 nM[21]	MeO	IC$_{50}$ 20 nM[21]
MeO	IC$_{50}$ 28 nM[21]	MeO	IC$_{50}$ 16 nM[21]
MeO	IC$_{50}$ 16 nM[21]	iPr, NEt$_2$	Ki 13 nM[23]
NEt$_2$	K_i 13 nM[23]	NEt$_2$	K_i 5.8 nM[23]
NEt$_2$	K_i 13 nM[23]	SMe	IC$_{50}$ 3.31 µM[24]
OPh, Ph	k_{obs}/[I] 144.2 M^{-1} s^{-1}[25]	Ph	K_i 4 M^{-1}s^{-1}[26]
Ph	K_i 768 M^{-1}s^{-1}[27]	OTBS, CO$_2$Et, OBn, OBn, OBn	K_i 0.7 µM[28]
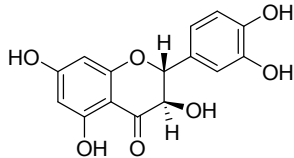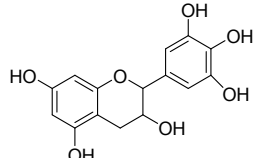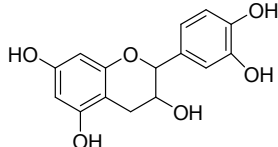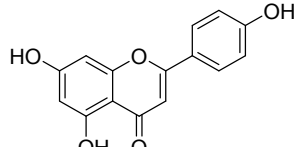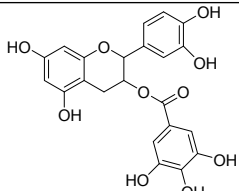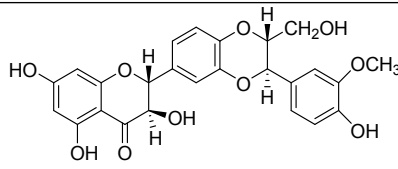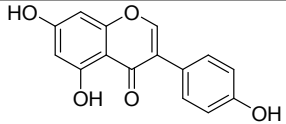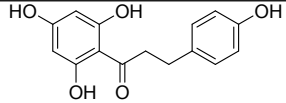
Compound	Activity[ref]	Compound	Activity[ref]
	IC_{50} 0.37 μM[29]		IC_{50} 0.010 μM[30]
	K_i 0.95 nM[31]		K_i 0.64 nM[11]
	IC_{50} 3.31 μM[32]		IC_{50} 0.081 μM[33]
	K_{inact}/K_i 1.0×10^6 M^{-1}s^{-1}[34]		K_{inact}/K_i 6.0×10^6 M^{-1}s^{-1}[34]
	K_{inact}/K_i 24700 M^{-1}s^{-1}[12]		K_i 7.34 μM[35]
	IC_{50} 6.7 μM[13]		IC_{50} 0.23 μM[36]
	IC_{50} 0.32 μM[14]		IC_{50} 0.03 μM[37]
	IC_{50} 0.032 μM[38]		IC_{50} 4.42 μM[39]
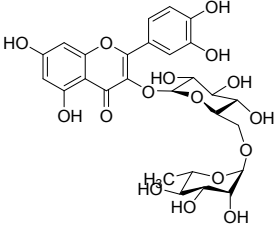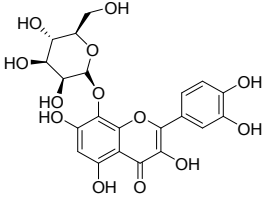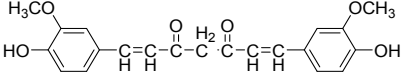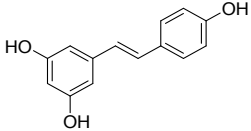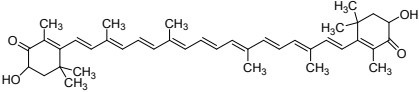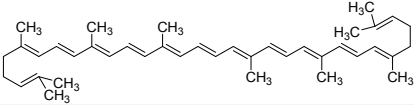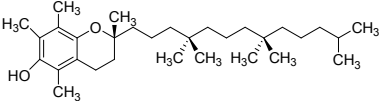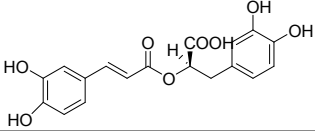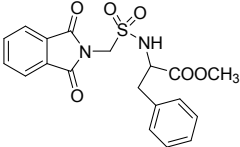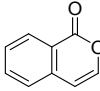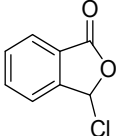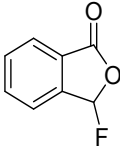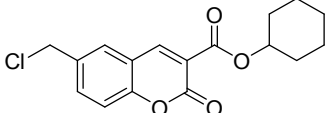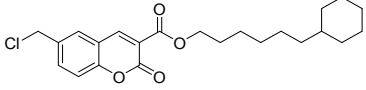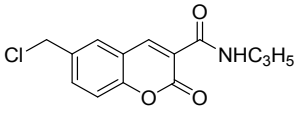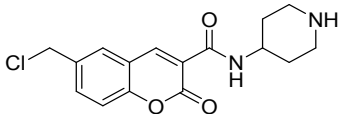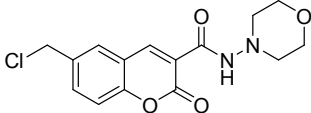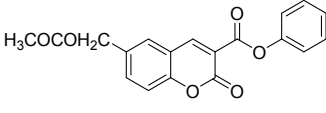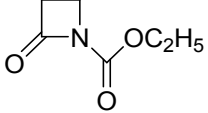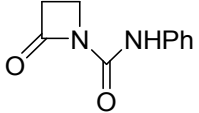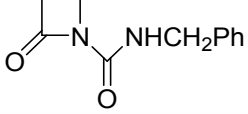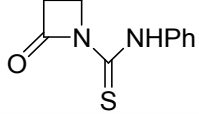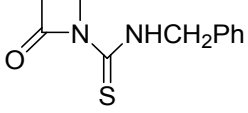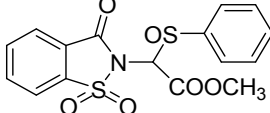
Compound	Activity[ref]	Compound	Activity[ref]
	IC$_{50}$ 2-4.42 µM[39]		IC$_{50}$ 2-4.42 µM[39]
	IC$_{50}$ 0.5 µM[40]		IC$_{50}$ 0.21 nM[41]
	IC$_{50}$ 0.9 nM[41]		IC$_{50}$ <15 nM[41]
	IC$_{50}$ <0.3 nM[41]		k_{obs}/[I] 7.5 x10^6 M^{-1}s^{-1}[41]
	IC$_{50}$ 600 nM [42]		IC$_{50}$ 170 nM[16]
	IC$_{50}$ 350 nM[43]		IC$_{50}$ 390 nM[42]
	IC$_{50}$ 635 nM[16]		IC$_{50}$ 710 nM[16]
	IC$_{50}$ 900 nM[16]		IC$_{50}$ 1000 nM[18]
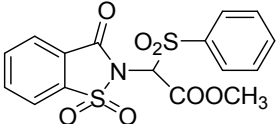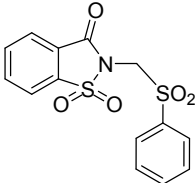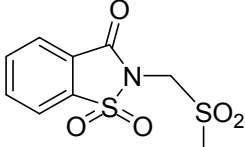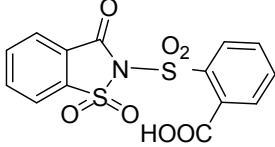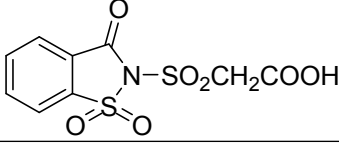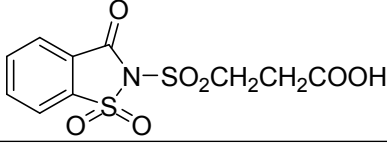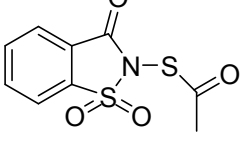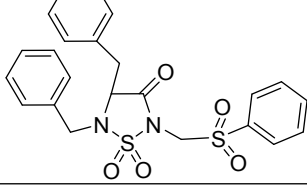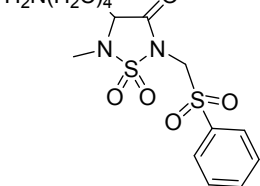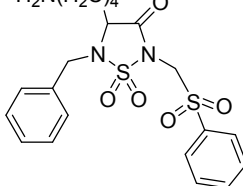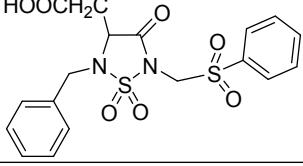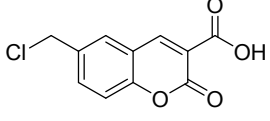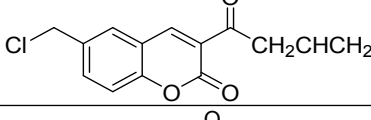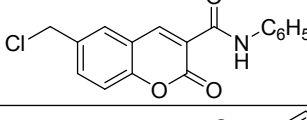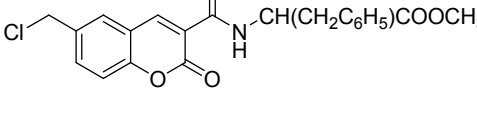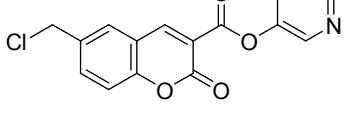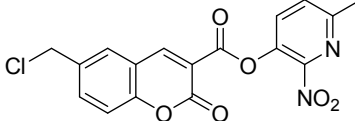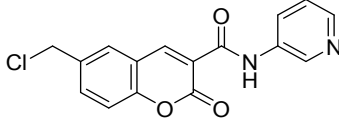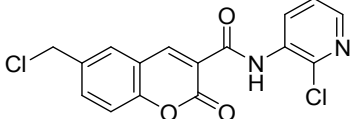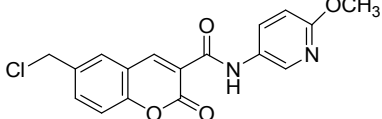
Compound	Activity[ref]	Compound	Activity[ref]
	IC$_{50}$ 5300 nM[16]		IC$_{50}$ 5000 nM[42]
	IC$_{50}$ 9300 nM[16]		IC$_{50}$ 9500 nM[44]
	K_{inact}/K_I 2.4x10^5 M^{-1}s^{-1}[34]		K_{inact}/K_I 9.3x10^4 M^{-1}s^{-1} [34]
	K_{inact}/K_I 3.5x10^4 M^{-1}s^{-1} [34]		K_{inact}/K_I 2.0x10^4 M^{-1}s^{-1} [34]
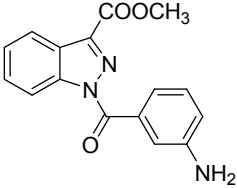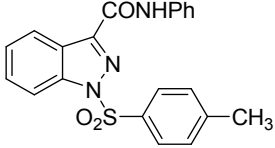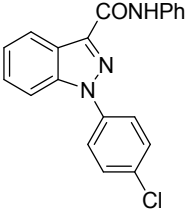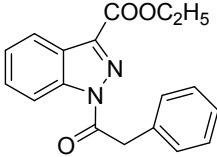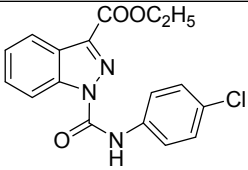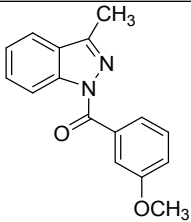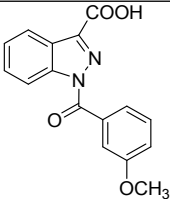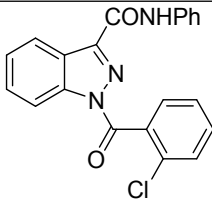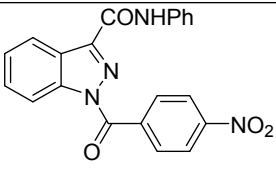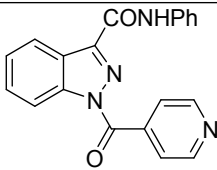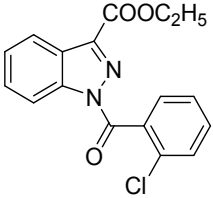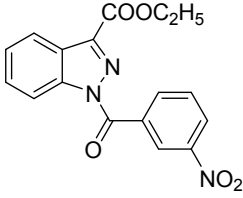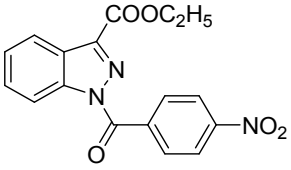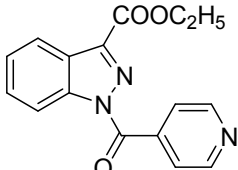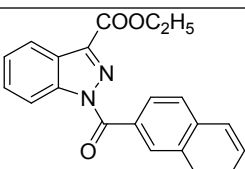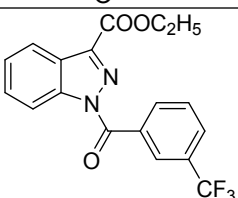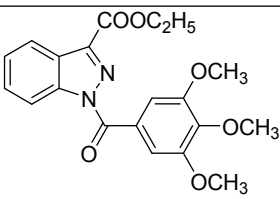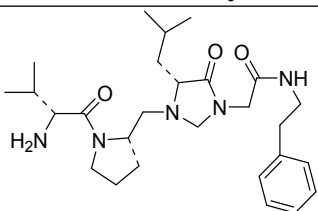
1.3 Pharmacophore Negative control Test Set
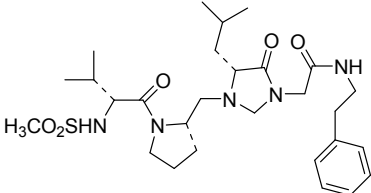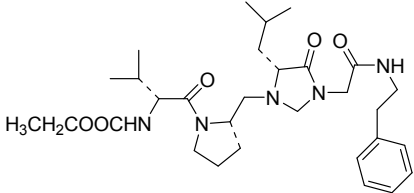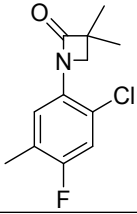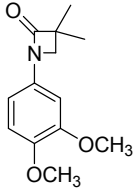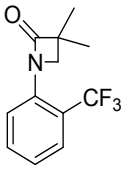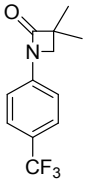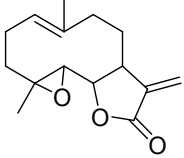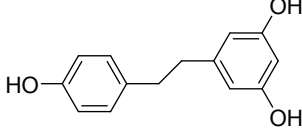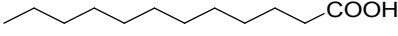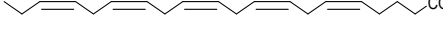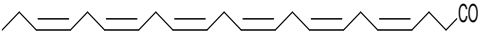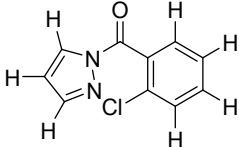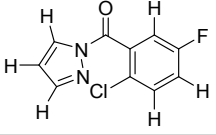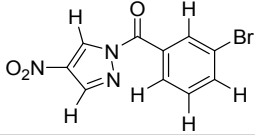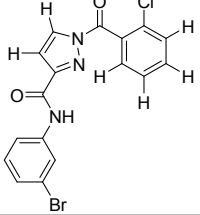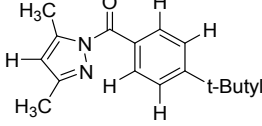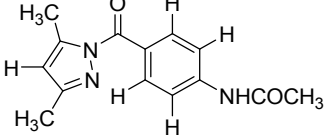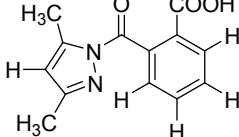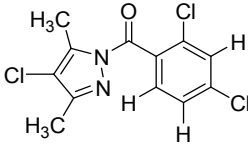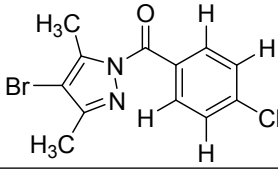
TableS2. Pharmacophore Negative Control Test Set
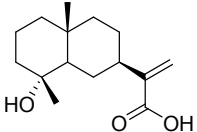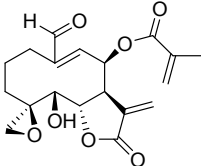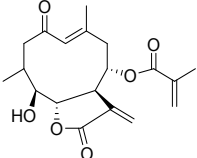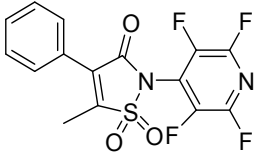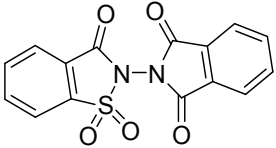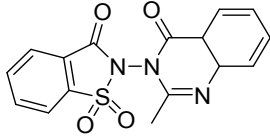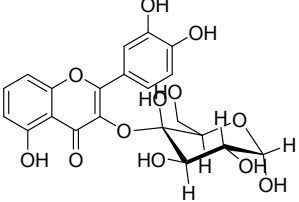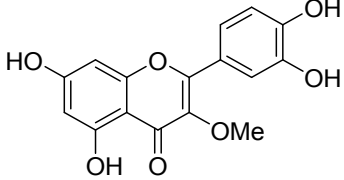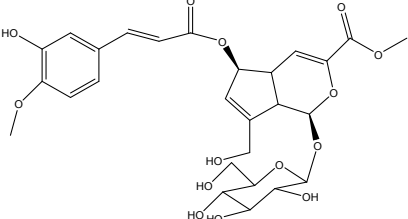
[Ref]	Compound	[Ref]	Compound
[45]		[46]	
[46]		[46]	
[46]		[46]	
[46]		[46]	

[Ref]	Compound	[Ref]	Compound
[46]	OH, OH, HO, HO, OH, OH, OH, OH, OH, O, H$_3$C, O, HO, OH, OH	[46]	OH, HO, HO, OH, HO, OH, HO, OH, OH, OH, O, O
[46]	H$_3$CO, HO, C=C, H, O, H$_2$, O, C=C, H, OCH$_3$, OH	[46]	HO, OH, OH
[46]	CH$_3$, CH$_3$, CH$_3$, H$_3$C, OH, O, HO, CH$_3$, CH$_3$, CH$_3$, CH$_3$, CH$_3$, CH$_3$, O	[46]	CH$_3$, CH$_3$, CH$_3$, H$_3$C, CH$_3$, CH$_3$, CH$_3$, CH$_3$, CH$_3$, CH$_3$
[46]	H$_3$C, CH$_3$, CH$_3$, CH$_3$, O, HO, H$_3$C, CH$_3$, H$_3$C, CH$_3$, CH$_3$, CH$_3$, CH$_3$, CH$_3$	[46]	OH, OH, COOH, H, O, HO, O, HO
[47]	O, S, O, O, N, NH, COOCH$_3$, O	[48]	O, O
[48]	O, O, Cl	[48]	O, O, F
[49]	Cl, O, O, O, O	[49]	Cl, O, O, O, O
[49]	Cl, O, NHC$_3$H$_5$, O, O	[49]	Cl, O, NH, H, NH, O, O
[49]	Cl, O, NH, N, O, O, O	[49]	H$_3$COCOCH$_2$C, O, O, O, O
[50]	O, N, OC$_2$H$_5$, O	[50]	O, N, NHPh, O
[50]	O, N, NHCH$_2$Ph, O	[50]	O, N, NHPh, S
[50]	O, N, NHCH$_2$Ph, S	[51]	O, N, OS, COOCH$_3$, S, O, O

[Ref]	Compound	[Ref]	Compound
[51]		[52]	
[51]		[51]	
[51]	N—SO₂CH₂COOH	[51]	N—SO₂CH₂CH₂COOH
[51]		[52]	
[52]		[52]	
[52]		[53]	
[53]		[53]	
[53]		[54]	
[54]		[54]	
[54]		[54]	

[Ref]	Compound	[Ref]	Compound

[Ref]	Compound	[Ref]	Compound
[56]		[56]	
[57]		[57]	
[57]		[57]	
[58]		[58]	
[58]		[58]	
[58]		[3]	
[3]		[3]	
[3]		[3]	
[3]		[3]	
[3]		[3]	

S14

[Ref]	Compound	[Ref]	Compound
[59]		[59]	
[59]		[33]	
[60]		[60]	
[13]		[61]	
[62]			

1.4 Methodology

A database containing the training set (Figure S1) was prepared using MOE software with known inhibitors. The compounds were then minimized using the MMFF force field to an energy gradient <0.00001 to create a 3D structural database.

Different pharmacophoric schemes were tested in order to pursuit the most representative features to be able to overlay active molecules while discriminating actives from inactives. This was performed by varying the training set (different groups of molecules from the training set at Figure S1 were assayed for alignment, Table S3) and the pharmacophoric model generation was performed using different alignment methodologies and pharmacophoric schemes (Table S3). Validation was performed against a test set containing structurally diverse HNE inhibitors with activities bellow 5 µM (n=106, positive control, Table S1) and a group of diverse molecules that when tested against HNE showed no inhibitory activity (n=99, negative control, Table S2).

Different pharmacophoric models using different annotation schemes were generated using available tools at MOE package (Table S3), with default parameters with maximum query feature number defined to 5.

A short description of the tools applied is given bellow:

1. Pharmacophoric Elucidator using Unified or PCHD annotation schemes

Pharmacophore Elucidator (**PE**) generates a collection of pharmacophoric queries from a collection of active compounds against a particular biological target so that feature geometries common to many of the actives will contain information related to the important interactions between the bound conformations of the actives and the receptor. Pharmacophore Elucidation accepts as input a collection of N molecules each with C_i conformations. A conformational search and import was performed in MOE to create a second database of HNE inhibitors that retained 100 of the lowest conformations for each inhibitor.

Pharmacophore Elucidation generates pharmacophore queries each of which matches at least *n* active molecules. Typically, and in our assays, *n* is 90% of the training set that contained only actives as these queries with a coverage of *n* are said to be *popular.* For each query, the 5 top scored pharmacophores were evaluated against the test set, and for all the cases the higher scored pharmacophore was the one that presented best results which are given in Table S3.

Different annotation schemes were used to generate the pharmacophoric hypothesis:

UNI-*Unified* annotation scheme: This is the most comprehensive and includes all of the annotation types defined in MOE (H-bond Donor, H-bond Donor Projection, H-bond Acceptor, H-bond Acceptor Projection, π *vs.* Non-π H-bond Donor/Acceptor, General π *vs.* Non-π Distinctions, Metal Ligator, Metal Ligator Projection, Cation, Anion, NCN+ Bioisostere, COO-Bioisostere, Aromatic Centroid, Aromatic Centroid Normal, π-Ring Centroid, π-Ring Centroid Normal, Hydrophobe, Hydrophobic Centroid, R-Group Link, R-Group Link Projection).

PCHD- Polar-Charged-Hydrophobic-Direccional scheme includes the following annotation points: H-bond Donor, H-bond Donor Projection, H-bond Acceptor, H-bond Acceptor Projection, Metal Ligator, Metal Ligator Projection, Cation, Anion, Aromatic Centroid, Aromatic Centroid Normal, Hydrophobic Centroid.

2. Flexible Alignment with phamacophoric consensus (FA/PC)

Flexible Alignment (**FA**) is a stochastic search procedure that simultaneously searches the conformation space of a collection of molecules and the space of alignments of those molecules. As a result, the method is asymptotically complete. The scoring of alignments is based upon a Gaussian density representation of features tuned to reproduce certain X-ray crystallographic alignments. MOE default conditions were used for the flexible alignment of the training set.

The Pharmacophore Consensus (**PC**) tool creates a list of suggested features from a set of aligned conformations, based on specified consensus parameters. Suggested features were converted to query features using MOE default tolerance radius (1.2), consensus score threshold (50%) and consensus score mode (weighted conformation).

Table S3. Pharmacophoric models and respective features, using different training sets and different annotation schemes, generated using available tools at MOE package and validated against the test set containing positive control (actives) and negative control (inactives).

Training Set	Ph	Method	Features	Radius	% Hits	
					Control +	Control -
S2-S11	1	PE/UNI	2 Hyd Acc2 Acc2	1.4 1 1	82	37
	2	PE/PCHD	Acc 2 Hyd/Aro Hyd/Aro Acc2	1 1.4 1.4 1	97	86
	3	PE/PCHD	Acc 2 Hyd Hyd Acc2	1 1.4 1.4 1	80	45
	4	FA/PC	Acc Acc Acc2 Acc2 PiN Hyd/Aro	0.62 0.74 0.66 0.69 0.74 0.75	25	16
	5	FA/PC	Acc Acc Acc2 Acc2 PiN Hyd	0.62 0.74 0.66 0.69 0.74 0.75	24	16
S1+ S12-S20	6	PE/PCHD	Acc Hyd/Aro Hyd/Aro Acc2	1 1.4 1.4 1	67	42
	7	PE/PCHD	Acc Hyd Hyd Acc2	1 1.4 1.4 1	53	18
	8	FA/PC	Aro/Hyd/Acc Acc/Don Aro/Hyd Acc2	2 1.7 1.7 1.1	97	87
	9	FA/PC	Acc Acc Aro Acc2	2 1.7 1.7 1.1	91	63
S1-S20	10	PE/PCHD	Acc Hyd/Aro Hyd/Aro Acc2	1 1.4 1.4 1	98	88
	11	PE/PCHD	Acc Hyd Hyd Acc2	1 1.4 1.4 1	80	45

Training Set	Ph	Method	Features	Radius	% Hits	
					Control +	Control -
S2-S16	12	PE/PCHD	Acc Hyd/Aro Hyd/Aro Acc2	1 1.4 1.4 1	99	83
	13	PE/PCHD	Acc Hyd Hyd Acc2	1 1.4 1.4 1	80	44
S2-S14	14	PE/PCHD	Acc Hyd/Aro Hyd/Aro Acc2 Acc2	1 1.4 1.4 1 1	100	79
	15	PE/PCHD	Acc Hyd Hyd Acc2 Acc2	1 1.4 1.4 1 1	80	34
S2-S13	16	PE/UNI	Hyd Hyd Acc2 Acc2	1.4 1.4 1 1	72	30
	17	PE/PCHD	Acc Hyd/Aro Hyd/Aro Acc2 Acc2	1 1.4 1.4 1 1	95	66
	18	PE/PCHD	Acc Hyd Hyd Acc2 Acc2	1 1.4 1.4 1 1	91	38
S2-S12	19	PE/UNI	Aro/PiR Hyd Hyd Acc2	1.4 1.4 1.4 1	63	28
	20	PE/UNI	Aro 2 Hyd Acc2	1.4 1.4 1.4 1	63	28
	21	PE/PCHD	Acc Hyd/Aro Hyd/Aro Acc2	1 1.4 1.4 1	99	85
	22	PE/PCHD	Acc Hyd Hyd Acc2	1 1.4 1.4 1	95	48

PE-pharmacophore elucidator; UNI-Unified; PCHD-Polar-Charged-Hydrophobic-Direccional; FA-Flexible Alignment; PC-Parmacophoric consensus; Hyd-hydrophobic; Acc-acceptor; Acc2-projected acceptor; Aro-aromatic; PiN-π-Ring Centroid; PiR-π-Ring Centroid.

After validation of the generated pharmacophoric models, Pharmacophore 18 (Table S3) was the one presenting higher discriminating power between active and inactive molecules, identifying 91% of the active molecules (positive control) as hits, while retrieves only 38% of the inactive molecules (negative control) as false positive hits. Hence, we proceed to the optimization of the pharmacophoric model, by applying iterative small changes of the radius and distances between the features. The changes applied to the distance between features did not led to significant improvement of the discrimination between actives and inactives, while changing the feature radius of Acc(F1, Figure S2), Hyd(F2, Figure S2), Hyd (F3, Figure S2), Acc2 (F4, Figure S2), Acc2 (F5, Figure S2) from 1, 1.4, 1.4, 1, and 1, to 0.5, 1.7, 1.5, 1.2 and 1.4, respectively, led to a slight improvement and the percentage of hits identified from the positive control (92%), while the false positive hits from the negative control set was slightly reduced to 35%. Hence, feature characterization for optimized pharmacophoric model is given in Figure S2.
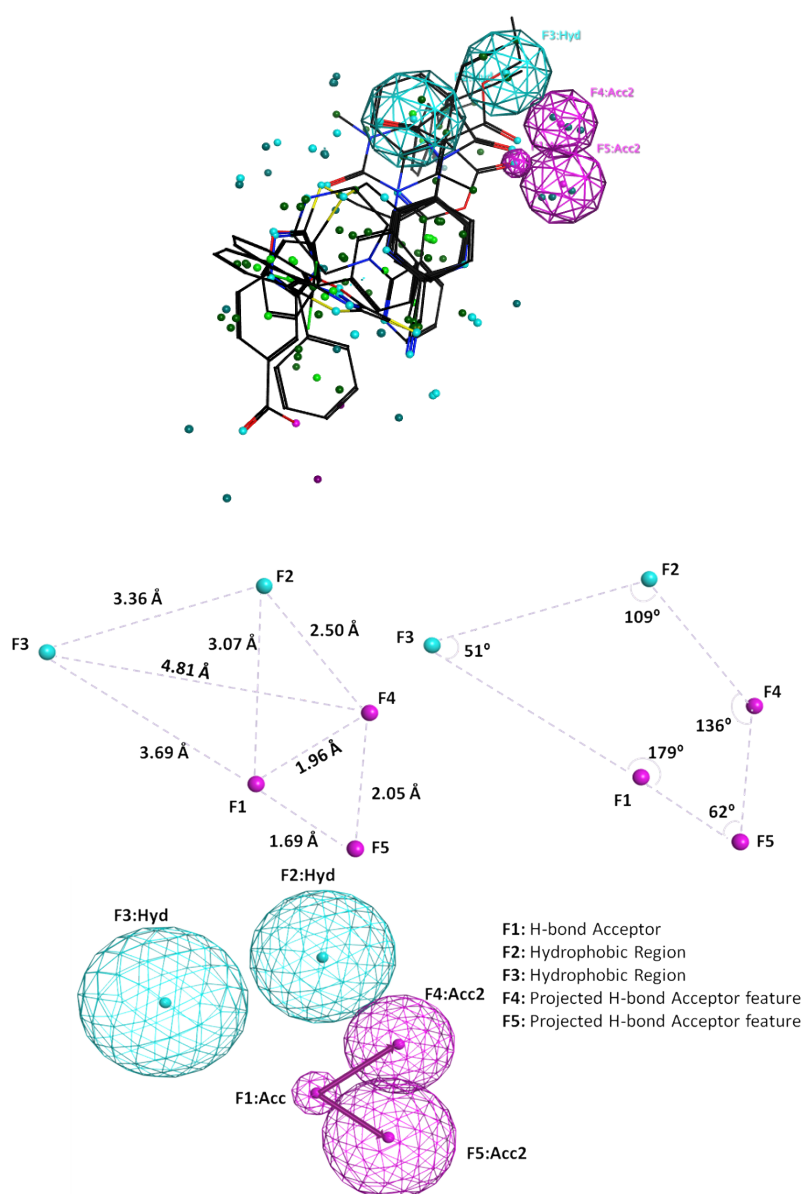
Figure S2. Optimized Pharmacophore model for HNE inhibition using MOE2012.10 software.

2   Molecular Docking

Three different 3D structure coordinates of HNE were obtained from the Protein Data Bank, PDB codes 3Q76, 3Q77 and 1HNE with X-ray coordinates at 1.86 Å, 2.00 Å and 1.84 Å resolution, respectively. To prepare the enzymes for the molecular docking studies, the co-crystallized inhibitor as well as crystallographic waters included in the PDB structure, were removed. Hydrogen atoms were added and the protonation states were correctly assigned using the Protonate-3D tool within the Molecular Operating Environment (MOE) 2012.10 software package, [63] energy was minimized using MMFF94x forcefield. Molecular docking studies were then performed using the GoldScore scoring function from GOLD5.1 software package[64] and each ligand was subjected to 500 docking runs. For complexed structures 3Q77 and 1HNE the docking methodology was validated using the crystallographic ligands and their poses were reproducible with RMSD lower than 0.8 Å.

The docking poses obtained for compound **1** show similar behavior when docked in a non-complexed HNE structure (Figure S3a) that presents a narrower shape of S1 pocket or when docked in HNE crystallographic structures that had co-crystallized inhibitors as 3Q77 (Figure S3b) or 1HNE (Figure S3c), indicating that the main contribution for its activity besides the oxo-β-lactam intrinsic reactivity is based on extra binding to S1 subsite by π-π stacking with Phe192, that may promote an induced-fit mechanism when getting close to HNE active-site.
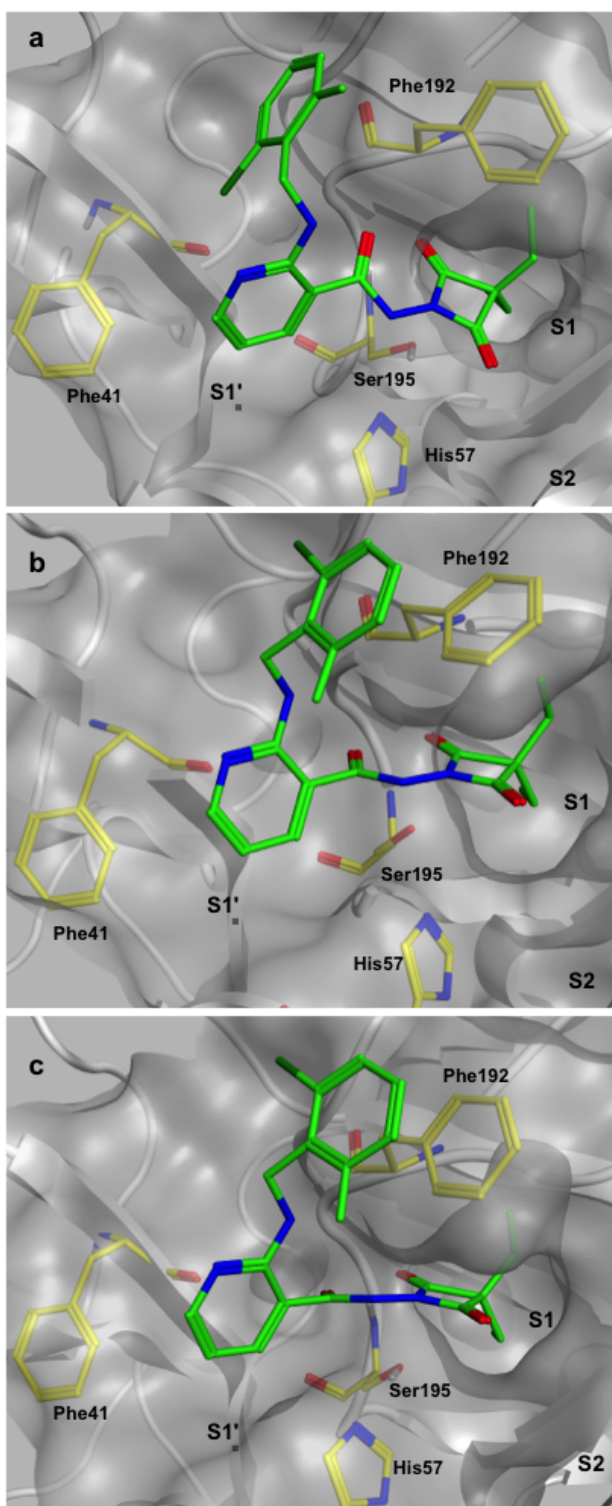
Figure S3 – Docking poses of compound **1** using different HNE coordinates, PDB 3Q76 (**a**), PDB 3Q77 (**b**) and PDB 1HNE (**c**).

3 Chemistry

3.1 General Considerations

Melting points (mp) were recorded on a Kofler camera Bock Monoscope M and are uncorrected.

Proton and carbon nuclear magnetic resonance (^{1}H and ^{13}C NMR) spectra were recorded on a Bruker Avance 400 (400 and 100 MHz, respectively). All chemical shifts are quoted on the δ scale in ppm using residual solvent peaks as the internal standard. Coupling constants (J) are reported in Hz with the following splitting abbreviations: s = singlet, d = doublet, t = triplet, q = quartet, dd = double doublet, m = multiplet.

Elemental analysis were performed in a Flash 2000 CHNS-O analyzer (ThermoScientific, UK).

Thin layer chromatography (TLC) was carried out using Merck aluminum backed sheets coated with 60 F254 silica gel. Visualization of the silica plates was achieved using a UV lamp (λ_{max} = 254 nm).

Flash chromatography was made using a Combi Flash RF-200 device from Teledyne Isco with RediSepbnormal-phase silica flash columns and using gradients of Hexane/EtOAc.

All reagents were purchased from Aldrich or AlfaAesar and used without further purification.

3.2 Synthesis
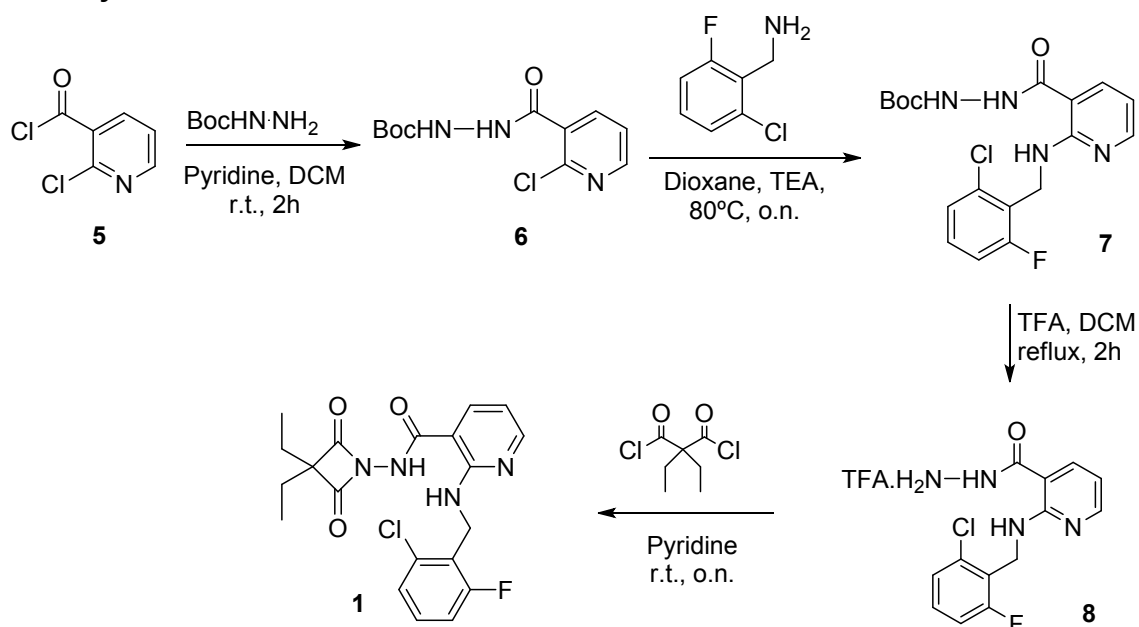
Scheme 1. Synthetic path for compound **1**.

tert-butyl 2-(3-chloroisonicotinoyl)hydrazinecarboxylate (6)

To a solution of *tert*-butoxycarbonyl hydrazide (667 mg, 5.05 mmol) in DCM (10 mL) and pyridine (0.5 mL) was added 2-chloropyridine-3-carbonyl chloride (1 g, 5.7 mmol) in DCM (10 mL) and the mixture was stirred at rt for 2h. The reaction mixture was diluted in DCM and washed with water, the organics were dried over anhydrous sodium sulfate, filtered and concentrated under reduce pressure. The residue was then recrystalized from diethyl ether to yield a white powder (1.3 g, 82%). ^{1}H-NMR δ 8.49 (dd, J = 4.6, 1.6 Hz, 1H, Ar), 8.13 (d, J = 7.2 Hz, 1H, Ar), 7.38 (dd, J = 7.5, 4.8 Hz, 1H, Ar), 6.94 (br s, 1H, NH), 1.51 (s, 9H, Boc).

tert-butyl 2-(3-((2-chloro-6-fluorobenzyl)amino)isonicotinoyl)hydrazinecarboxylate (7)

To a solution of compound **6** (100 mg, 0.37 mmol) in dry dioxane (2 mL) and TEA (2.22 mmol, 0,31 mL) was added under nitrogen 2-chloro-6-fluorobenzylamine (0.41 mmol, 0,048 mL) and the mixture was stirred at 80 °C, overnight. The mixture was washed with diluted HCl and the product extracted with 3x EtOAc, the organic were combined, dried over anhydrous sodium sulfate, filtered and concentrated under reduced pressure. The residue was purified by column chromatography on silica gel using EtOAc/n- hexane gradient as eluent and then recrystalized from hexane to yield a white powder (111 mg, 76%,)**.** ^{1}H-NMR δ 8.55 (s, 1H), 8.28 (s, 1H), 8.00 (s, 1H), 7.32 – 7.17 (m, 3H), 7.04 (d, J = 8.5 Hz, 1H), 6.69 (d, J = 31.2 Hz, 2H), 4.91 (d, J = 3.3 Hz, 2H), 1.46 (s, 9H).

3-((2-chloro-6-fluorobenzyl)amino)isonicotinohydrazide (8)

Trifluoroacetic acid (3 mL) was added under nitrogen to a solution of compound **7** (300 mg, 0.76 mmol), in dry DCM (30 mL) and the mixture was refluxed for 2h. The remaining TFA was co-evaporated with 3xDCM and the residue was then recrystalized from diethyl ether to yield the desired product as colorless crystals (224 mg, 78%). δ ^{1}H NMR (400 MHz, MeOD) 7.58 (d, J = 4.8 Hz, 1H), 7.44 (d, J = 6.8 Hz, 1H), 7.33 (d, J = 6.8 Hz, 1H), 6.66 (m, 1H), 6.57 (m, 2H), 6.36 (t, J = 7.1 Hz, 1H), 6.05 (t, J = 6.1 Hz, 1H), 4.16 (d, J = 7.2 Hz, 2H), 2.67 (s, 11H).

2-((2-chloro-6-fluorobenzyl)amino)-*N*-(3,3-diethyl- azetidin-1-yl -2,4-dione)nicotinamide (1)

To a solution of diethylmalonyl dichloride (1.88 mmol, 324 µL) in pyridine (3 mL) under nitrogen atmosphere was added a solution compound **8** (1.88 mmol, 768 mg) in pyridine (3 mL), dropwise, and the reaction proceeded overnight at room temperature. Pyridine was co-evaporated with 3x toluene. The residue was purified by flash chromatography on silica gel using EtOAc/n- hexane gradient as eluent and after recrystalization from hexane the desired product was obtained as colorless crystals (16 mg, 2%) mp 156-158 °C; δ ^{1}H NMR (400 MHz, CDCl3) 8.35-8.31 (m, 1H), 8.19 (s, 1H), 7.66 (d, J = 7.7 Hz, 1H), 7.23 (m, 2H), 7.05 – 6.99 (m, 1H), 6.53 (dd, J = 7.8, 4.8 Hz, 1H), 4.89 (d, J = 5.3 Hz, 2H), 1.88 (q, J = 7.5 Hz, 4H), 1.10 (t, J = 7.1 Hz, 6H). ^{13}C NMR (101 MHz, CDCl3) δ 204.4 (C2,4), 174.2 (C8), 165.5 (Pyr6), 157.4 (Ar2), 153.6 (Pyr4), 136.0 (Pyr2), 129.4 (Ar6), 125.4 (Ar1), 124.5 (Pyr4), 114.4 (Pyr2), 114.1 (Ar4), 110.9 (Ar5), 105.4 (Ar3), 66.9 (C3), 36.32 (C10), 23.4 (C5), 9.2 (C6). Calcd. ($C_{20}H_{20}ClFN_4O_3$): C, 57.35; H, 4.81; N, 13.38%. Found: C, 57.14; H, 4.81; N, 13.65%. Crystallographic Data for **1** is presented in section 3.4.

N-(3,3-diethyl-azetidin-1-yl -2,4-dione)benzamide (2)

To a solution of diethylmalonate dichloride (3.67 mmol, 0.63 mL) in pyridine (5 mL) was added dropwise a solution of N-benzoyl-hydrazine (0.5 g, 3.67 mmol) in pyridine (5 mL), under stirring and nitrogen atmosphere. The reaction was stirred at room temperature overnight. Pyridine was co-evaporated with 3x toluene. The resulting residue was dissolved in dichloromethane and washed three times with water, the organic phase was dried with anhydrous magnesium sulfate and filtered and concentrated under reduced pressure. The obtained residue was purified by flash chromatography on silica gel to afford the desired product as a colorless solid (0.220 g, 23%) mp 116-119 °C; ^{1}H-NMR (400 MHz, CDCl$_3$), δ(ppm): 1.13 (6H, t, J = 7.1 Hz, 2CH$_3$), 1.88 (4H, q, J = 7.8 Hz, 2CH$_2$), 7.46 (2H, t, J = 7.7 Hz, Ar), 7.58 (1H, t, J = 7.1 Hz, Ar), 7.78 (2H, d, J = 7.1 Hz, Ar), 8.49 (1H, s, NH); ^{13}C-NMR (100 MHz, CDCl$_3$), δ(ppm): 174.1, 165.1, 133.2, 130.0, 128.9, 127.6, 67.2, 23.6, 9.3. Calcd. (C$_{14}$H$_{16}$N$_2$O$_3$): C, 64.60; H, 6.20; N, 10.76%. Found: C, 65.07; H, 6.40; N, 10.51%.

N-(3,3-diethyl-azetidin-1-yl-2 ,4-dione)-4-methylbenzenesulfonamide (3)

To a solution of dimethylmalonate chloride (3.9 mmol, 0.67 mL) in pyridine (5 mL) under stirring and nitrogen atmosphere at 5 °C (ice-water bath) was added dropwise a solution of p-toluenesulfonyl hydrazine (3.9 mmol, 0.73 g) in pyridine (5 mL). The reaction was stirred at room temperature overnight. Pyridine was co-evaporated with 3x toluene. The resulting residue was dissolved in dichloromethane and washed three times with water, the organics were dried with anhydrous magnesium sulfate and filtered and concentrated under reduced pressure. The obtained residue was purified by silica gel chromatography (EtOAc/n-hexane (1:3)) to afford the desired product as a colorless solid (10%), mp 129-131 °C; ^{1}H-NMR (DMSO): 0.85 (6H, t, J = 7.2 Hz, 2CH$_3$), 1.62 (4H, q, J = 7.2 Hz, 2CH$_2$), 2.39 (3H, s, Ar-CH$_3$), 7.45 (2H, d, J = 7.6 Hz, Ar-H), 7.73 (2H, d, J = 7.6 Hz, Ar-H); 11.45 (1H, s, NH); ^{13}C-NMR (DMSO): 9.2 (2CH$_3$), 21.5 (CH$_3$), 23.2 (2CH$_2$), 66.3 (Cq), 127.8 and 130.1 (Ar, C2, C3, C5, C6), 136.1 (Cq, Ar-C4), 145.0 (Cq, Ar-C1), 173.20 (2Cq C=O). Crystallographic Data for **3** is presented in section 3.4.

N-(3,3-diethyl-azetidin-1-yl-2 ,4-dione)-N,4-dimethylbenzenesulfonamide (4)

To a solution of diethylmalonyl dichloride (2.6 mmol, 450 µL) in dioxane (20 mL) under nitrogen atmosphere was added a solution N-methyl-tosylhydrazine (2.6 mmol, 525 mg) in dioxane (20 mL), dropwise, followed by a solution of TEA (985 µL) in dioxane (20 mL). The reaction was stirred at room temperature overnight. The reaction mixture was concentrated and the obtained residue was purified by flash chromatography on silica gel using EtOAc/n-hexane gradient as eluent and after recrystalization from hexane the desired product was obtained as colorless crystals colorless solid (0.168 g, 21%). ^{1}H-NMR (400 MHz, CDCl$_3$) δ(ppm): 7.78 (d, J = 8.2 Hz, 2H, Ar), 7.36 (d, J = 8.1 Hz, 2H, Ar), 3.22 (s, 3H, NCH$_3$), 2.46 (s, 3H, Ar-CH$_3$), 1.76 (q, J = 7.5 Hz, 4H, 2CH$_2$), 1.02 (t, J = 7.5 Hz, 6H, 2CH$_3$). ^{13}C-NMR (100 MHz, CDCl$_3$) δ(ppm): 172.7, 145.5, 132.9, 130.0, 128.6, 66.4, 38.0, 23.6, 21.8, 9.1. Anal. Calcd. (C$_{15}$H$_{20}$N$_2$O$_4$S): C, 55.54; H, 6.21; N, 8.64%; S, 9.88%. Found: C, 55.38; H, 6.19; N, 8.57%; S, 9.65%.

3.2 NMR Spectra for compounds 1-4

¹H-NMR (400MHz, CDCl₃) for compound **1**:
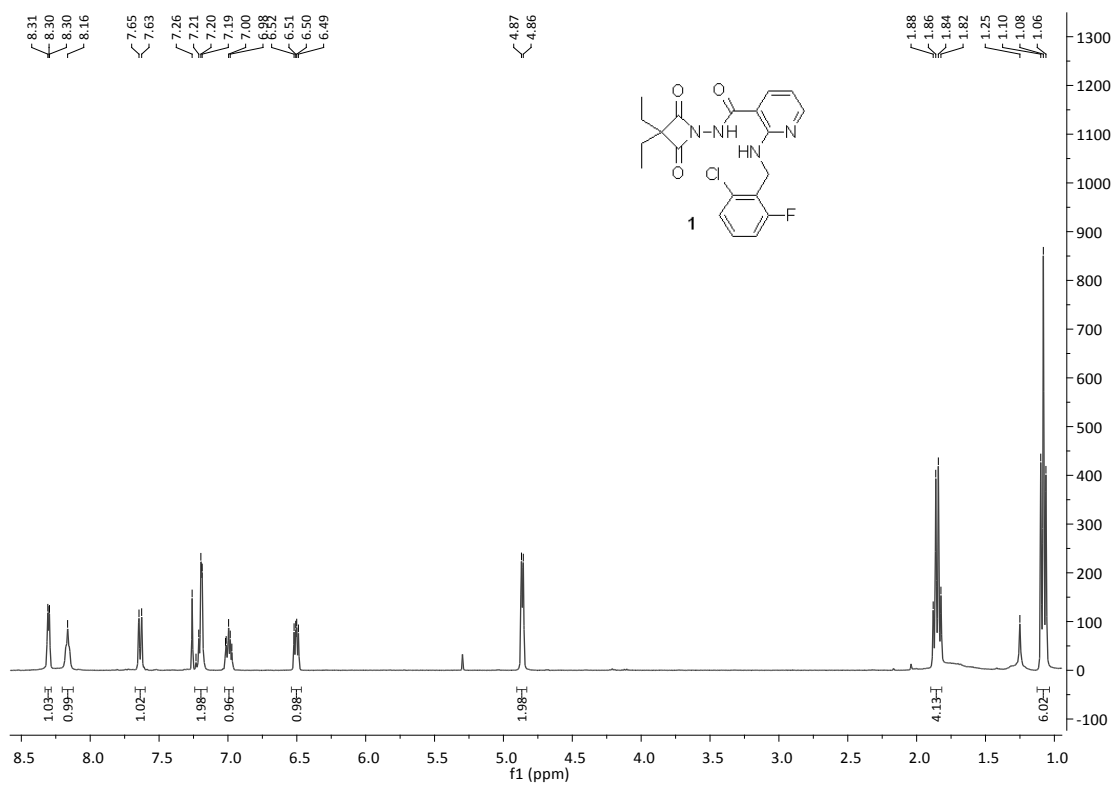
¹³C-NMR (100MHz, CDCl₃) for compound **1**:

¹H-NMR (400MHz, CDCl₃) for compound **2**:
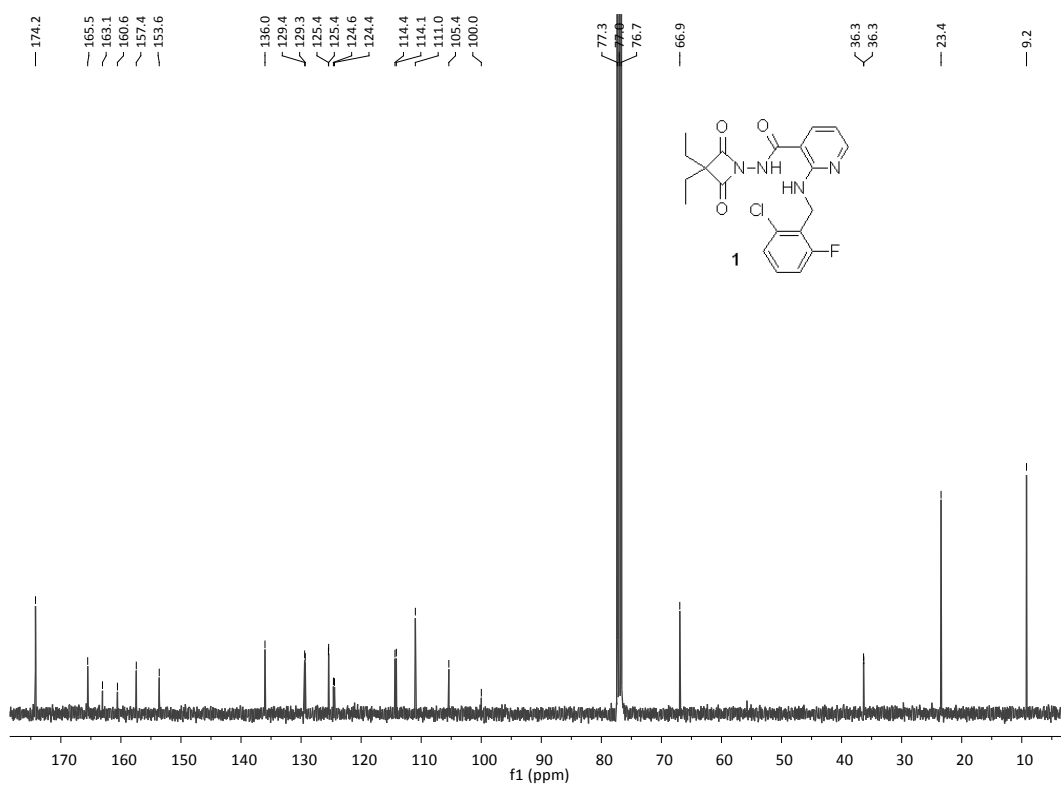
^{1}H-NMR (400MHz, CDCl$_3$) for compound **2**:
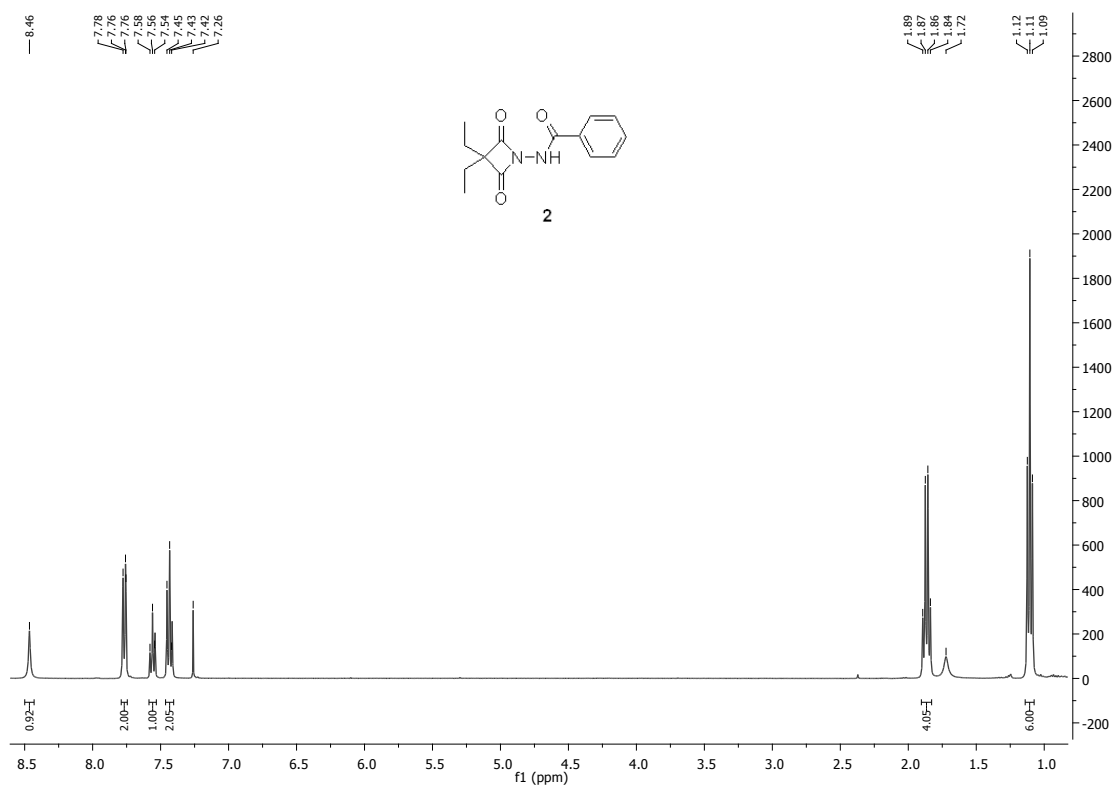
^{13}C-NMR (100MHz, CDCl$_3$) for compound **2**:
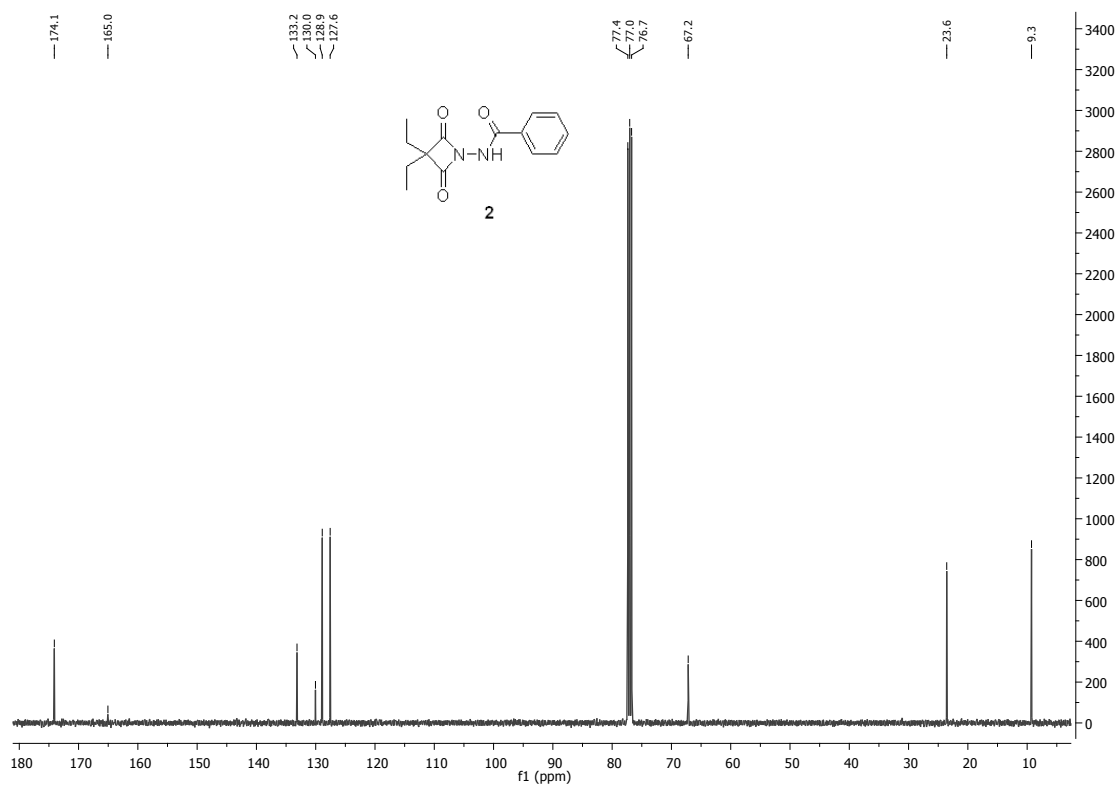
¹H-NMR (400MHz, CDCl₃) for compound **3**:
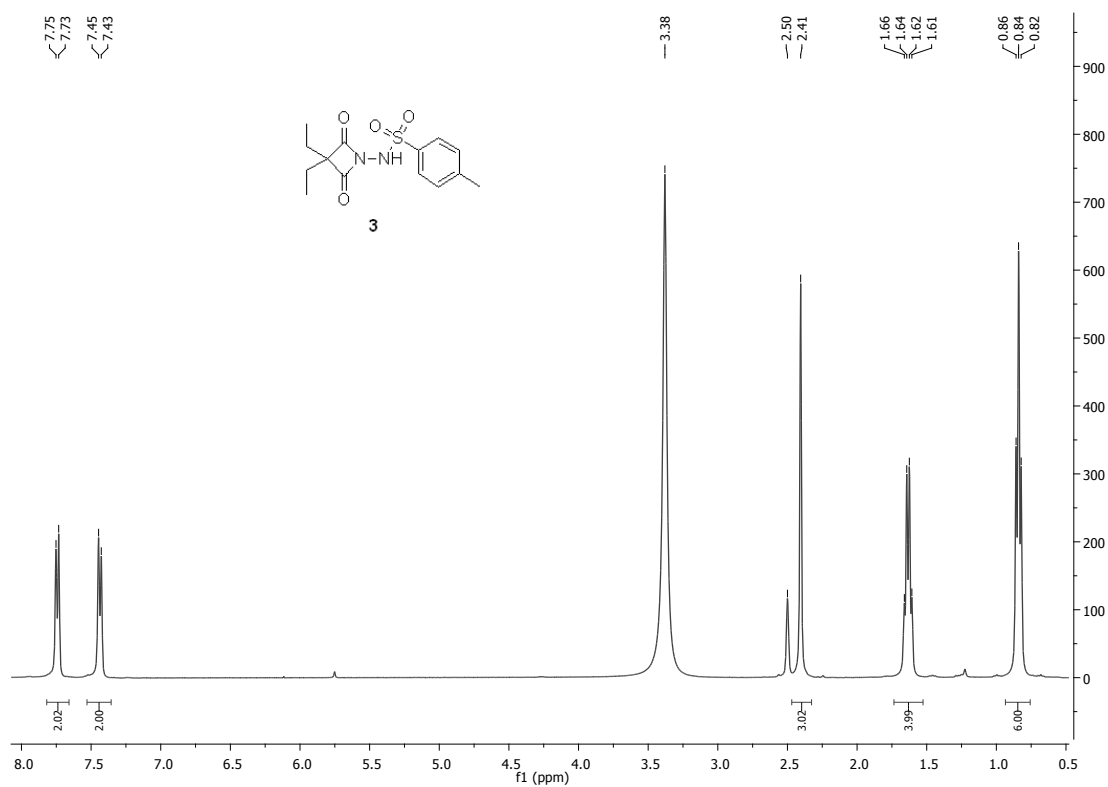
¹³C-APT-NMR (100MHz, CDCl₃) for compound **3**:
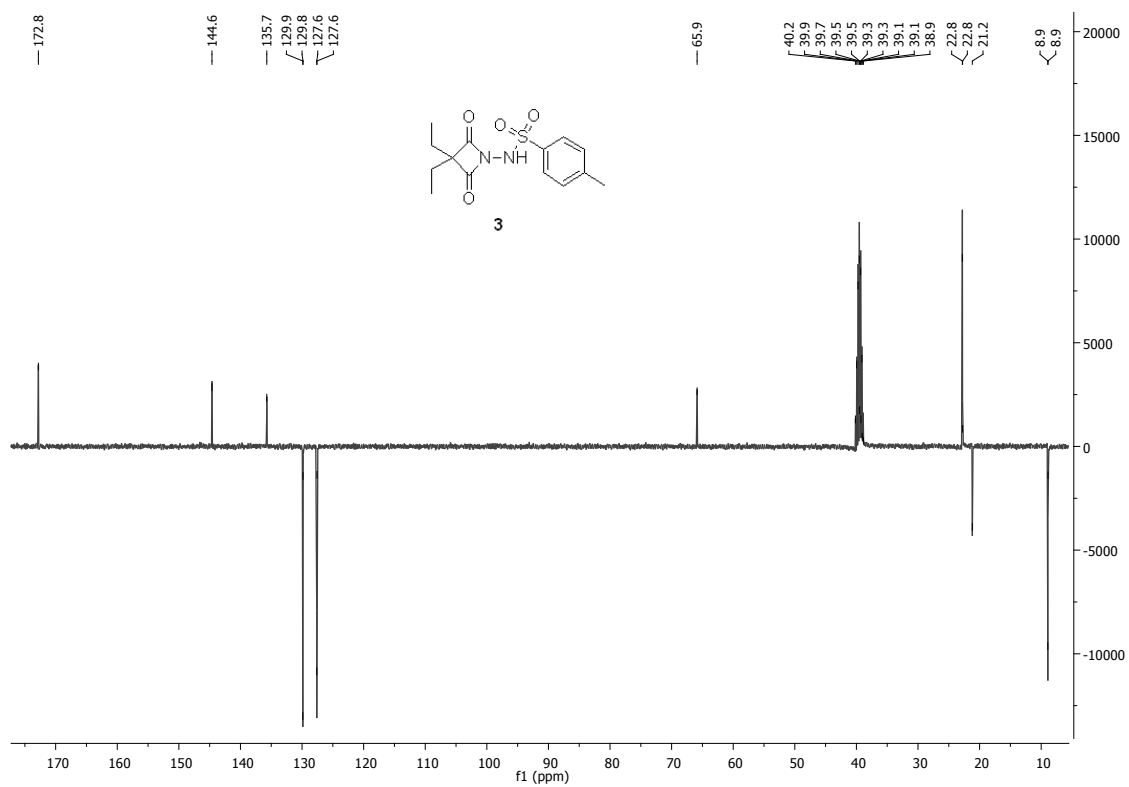
^{1}H-NMR (400MHz, CDCl$_3$) for compound **4**:
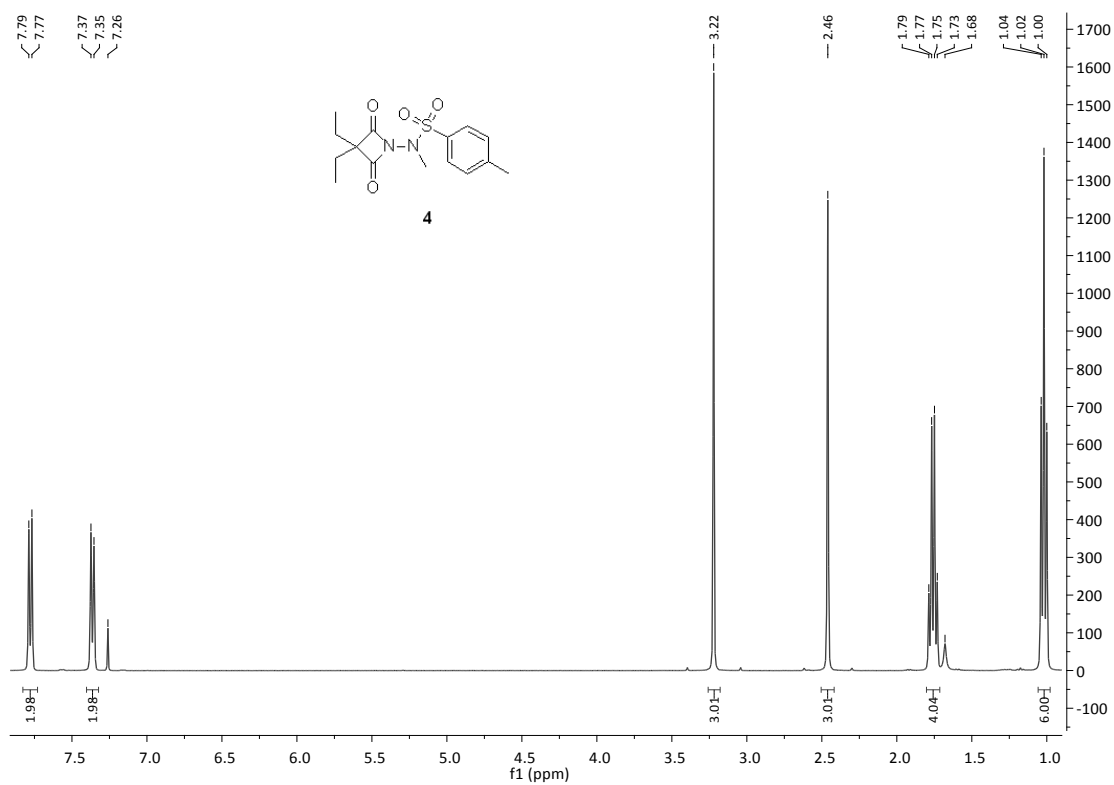
^{13}C-NMR (100MHz, CDCl$_3$) for compound **4**:
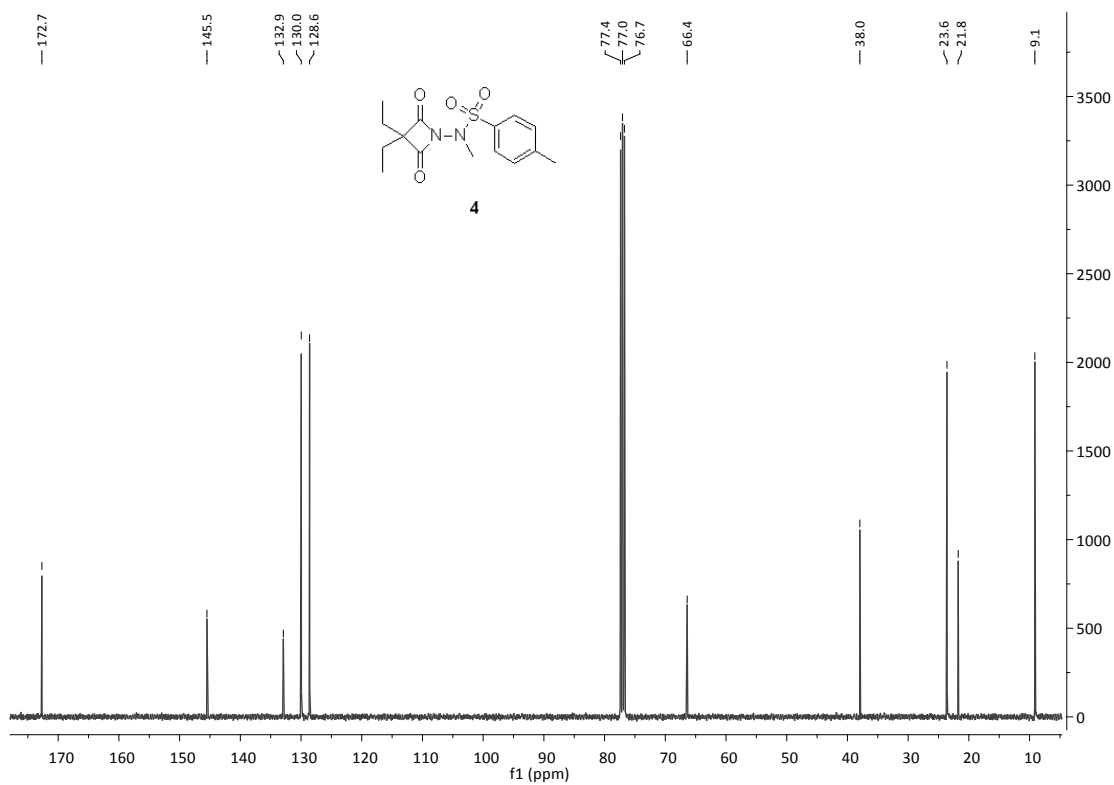
3.4 Solid state structural characterization of compounds 1 and 3
Crystallographic Data for compounds 1 and 3 (CCDC 1022848-1022849):

Crystals of **1** and **3** suitable for X-ray diffraction study were mounted with Fomblin© in a cryoloop. Data was collected on a Bruker AXS-KAPPA APEX II diffractometer with graphite-monochromated radiation (Mo Kα, λ=0.17073 Å) at 150 K. The X-ray generator was operated at 50 kV and 30 mA and the X-ray data collection was monitored by the APEX2 program. All data were corrected for Lorentzian, polarization and absorption effects using SAINT[65] and SADABS[66] programs. SIR97[67] and SHELXS-97[68] were used for structure solution and SHELXL-97 was applied for full matrix least-squares refinement on F^2. These three programs are included in the package of programs WINGX-Version 1.80.05.[69] Non-hydrogen atoms were refined anisotropically. A full-matrix least-squares refinement was used for the non-hydrogen atoms with anisotropic thermal parameters. All the hydrogen atoms were inserted in idealized positions and allowed to refine in the parent carbon or oxygen atom, except for the hydrogen atoms connected to nitrogen that were located from the electron density map and allowed to refine.
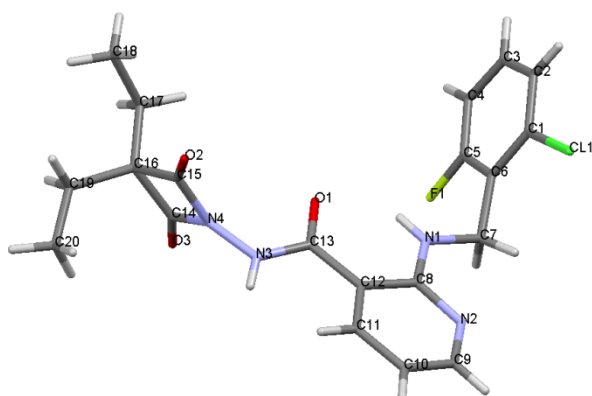
Figure S4 – Molecular structure for compound **1**
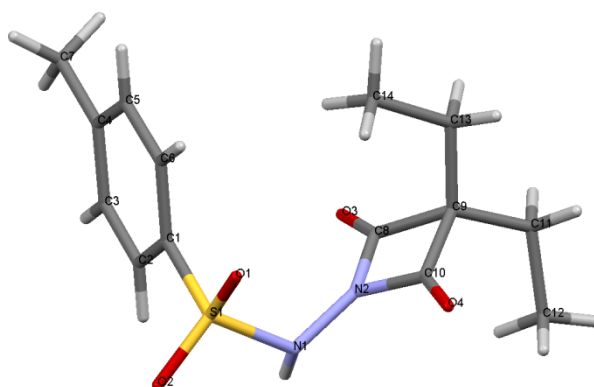
Figure S5 – Molecular structure for compound **3**

Table S4. Crystal Data and Structure Refinement Details for Compounds 1 and 3.

	1	3
formula	$C_{20}H_{20}Cl_1F_1N_4O_3$	$C_{14}H_{18}N_2O_4S$
fw	418.85	310.36
crystal form, color	plate, colorless	block, colorless
crystal size (mm)	0.20×0.08×0.01	0.2×0.10×0.10
crystal syst.	Orthorhombic	Orthorhombic
space group	$Pna2_1$	$P2_12_12_1$
a, Å	22.318(4)	6.702(3)
b, Å	10.108(3)	11.902(6)
c, Å	9.029(7)	18.892(4)
Z	4	16
V, Å^3	2036.9(17)	1507.0(11)
T, K	298(2)	150(2)
D_c, g cm^{-3}	1.366	1.367
μ(Mo Kα), mm^{-1}	0.225	0.232
θ range (°)	2.72–26.37	2.02–32.22
refl. collected	25820	19864
independent refl.	4092	5265
R_{int}	0.0397	0.0621
R_1[a], wR_2[b] $[I \geq 2\sigma(I)]$	0.0812, 0.02212	0.0416, 0.0948
GOF on F^2	1.059	1.007

[a] $R_1 = \Sigma||F_o| - |F_c||/\Sigma|F_o|$. [b] $wR_2 = [\Sigma[w(F_o^2 - F_c^2)^2]/\Sigma[w(F_o^2)^2]]^{1/2}$

4 Pharmacological Assays

For all serine proteases (human neutrophil elastase, porcine pancreatic elastase, cathepsin G, proteinase 3, thrombin, kallikrein, urokinase, trypsin and chymotrypsin), activity was monitored at 25 °C for 30 min at excitation and emission wavelengths of 360 and 460 nm, respectively in a microplate reader (FLUOstar Omega, BMG Labtech, Germany). For all compounds tested, the concentration of inhibitor that caused 50% inhibition of the enzymatic reaction (IC$_{50}$) was determined by non-linear regression using GraphPad PRISM software. Inhibitors stock solutions were prepared in DMSO, and serial dilutions were made in DMSO. Assays were performed in triplicate and data presented as the mean and the standard deviation.

4.1 Inhibition Assay for human neutrophil elastase

Fluorometric assays for the human neutrophil elastase (HNE, Merck, Germany) inhibition activity were carried out in 200 μL assay buffer (0.1 M HEPES pH 7.5 at 25 °C) containing 20 μL of 0.17 μM HNE in assay buffer (stock solution 1.7 μM in 0.05 M acetate buffer, pH 5.5), 155 μL of assay buffer and 5 μL of each concentration of tested inhibitors. After 30 min of incubation at 25 °C the reaction was initiated by the addition of 20 μl of fluorogenic substrate to final concentration 200 μM (MeO-Suc-Ala-Ala-Pro-Val-AMC, Merck, Germany). The K_m of this substrate of HNE was previously determined to be 185 μM (data not shown). For all assays, saturated substrate concentration was used, throughout, in order to obtain linear fluorescence curves. Controls were performed using enzyme alone, substrate alone, enzyme with DMSO and a positive control (Sivelestat sodium salt hydrate, Sigma Aldrich, UK).
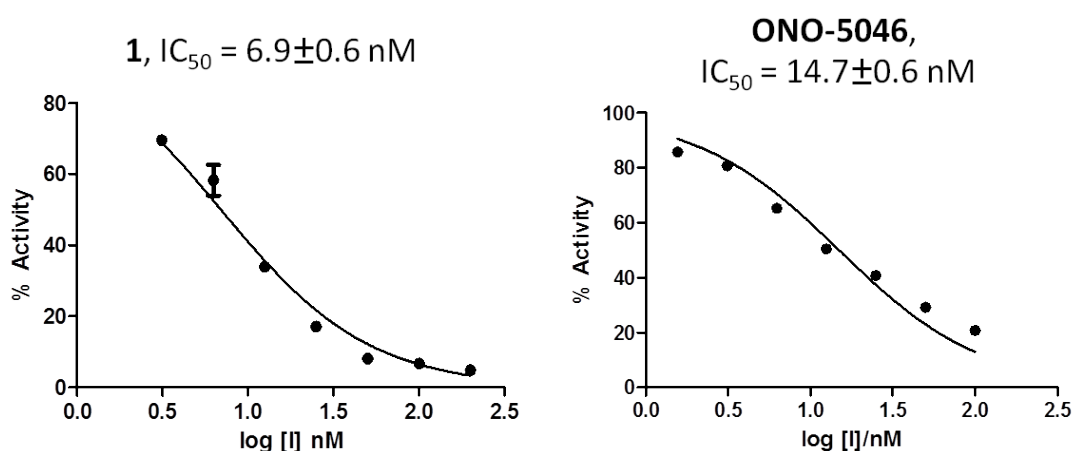
Figure S6. Inhibition curves for compound **1** and ONO-5046. Prepared using GraphPad Software.

4.2 Inhibition Assay for porcine pancreatic elastase

The inhibition of PPE was assayed by incubation method, 5 μl of inhibitor solution in DMSO was incubated at 25 °C with 155 μL of 0.1 M HEPES buffer, pH 7.5, and 20 μL of PPE solution (50 μM in 0.1 M HEPES buffer, pH 7.5). After 30min of incubation at 25 °C the reaction was initiated by the addition of 20 μL of fluorogenic substrate to final concentration of 200 μM (MeO-Suc-Ala-Ala-Pro-Val-AMC, Merck, Germany). Controls were performed using enzyme alone, substrate alone and enzyme with DMSO and positive control (Elastase Inhibitor I, # 324692, CalBiochem).

4.3   Inhibition Assay for proteinase 3

Inactivation of proteinase 3 (Calbiochem cat #539483) was studied at 25 °C in 200 µL assay buffer (0.1 M HEPES pH 7.5 at 25 °C) containing 70 µL of 65 nM proteinase 3 in assay buffer (stock solution 650 nM in 0.05 M acetate buffer, 150 mM NaCl, pH 5.5), 50 µL assay buffer and 5 µL of each concentration of tested inhibitors. The reaction was initiated by the addition of 75 µL of 10 mM chromogenic substrate (N-MeOSuc-Ala-Ala-Pro-Val-p-nitroanilide, stock solution 50 mM in DMSO, Sigma, UK) in assay buffer. Controls were performed using enzyme alone, substrate alone, enzyme with DMSO and a positive control.

4.4   Inhibition Assay for cathepsin G

Inactivation of cathepsin G (Calbiochem cat # 219373) was studied at 25 °C using the progress curve method. A Chromogenic 96 well microplate assay for the Cathepsin G, Human Neutrophil (Calbiochem, Germany) inhibition activity was carried out in 200 µL assay buffer (0.1 M HEPES pH 7.5 at 25 °C) containing 5 µL of each concentration of tested inhibitors, 125 µL of assay buffer and 20 µL of 680 nM Cathepsin G (680 nM in 0.05 M acetate buffer, pH 5.5). After a period of 30 minutes of incubation at 25 °C the reaction was initiated by the addition of 50 µL of 3.4 mM chromogenic substrate (Suc-Ala-Ala-Pro-Phe-p-nitroanilide, Calbiochem, Germany) in assay buffer (stock solution 42.5 mM in DMSO). Controls were performed using enzyme alone, substrate alone, enzyme with DMSO and a positive control (Cathepsin G inhibitor I, Calbiochem, Germany).

4.5   Inhibition Assay for urokinase

The analysis of urokinase (Calbiochem) inhibition assay was performed in reaction mixtures containing 0.05 M Tris-HCl, 0.138 M NaCl, pH 8.0, 30 U/mL human urine urokinase, test compounds, and 50 µM substrate (Z-Gly-Gly-Arg-AMC.HCl, Calbiochem). Controls were performed using enzyme alone, substrate alone, enzyme with DMSO and a positive control.

4.6   Inhibition Assay for kallikrein

The analysis of kallikrein (Calbiochem) inhibition was performed in reaction mixtures containing 0.05 M Tris-HCl, 0.138 M NaCl, pH 8.0, 2 nM human plasma kallikrein, test compounds, and 50 µM substrate (H-Pro-Phe-Arg-AMC acetate salt, Bachem). Controls were performed using enzyme alone, substrate alone, enzyme with DMSO and a positive control (Gabexate mesylate, Aldrich).

4.7   Inhibition Assay for thrombin

Inactivation of thrombin (Calbiochem) was studied at 25 °C in reaction mixtures containing 0.01 M sodium phosphate, 0.138 M NaCl, 0.1% PEG 6000, pH 7.0, 1.7 U/mL human plasma thrombin, test compounds, and 50 µM substrate (Z-Gly-Gly-Arg-AMC.HCl, Bachem). Controls were performed using enzyme alone, substrate alone, enzyme with DMSO and a positive control (3,4-Dichloroisocoumarin, Calbiochem, Germany).

4.8   Inhibition Assay for trypsin

The analysis of trypsin (Calbiochem) inhibition was performed in reaction mixtures containing 0.05 M Tris-HCl, 0.138 M NaCl, pH 8.0, 30 nM human pancreas trypsin, test compounds, and 50 µM substrate (Z-Gly-Gly-Arg-AMC.HCl, Bachem). Controls were performed using enzyme

alone, substrate alone, enzyme with DMSO and a positive control (3,4-Dichloroisocoumarin, Calbiochem, Germany).

4.9   Inhibition Assay for chymotrypsin

Inactivation of chymotrypsin (Calbiochem) was studied at 25 ºC in reaction mixtures containing 0.05 M Tris-HCl, 0.138 M NaCl, pH 8.0, 30 nM human pancreas chymotrypsin, test compounds, and 100 μM substrate (Suc-Ala-Ala-Pro-Phe-7-amino-4-methylcoumarin, Bachem). Controls were performed using enzyme alone, substrate alone, enzyme with DMSO and a positive control (Gabexate mesylate, Aldrich).

4.10 In Vitro Cytotoxicity

The cytotoxicity was assessed using general cell viability endpoint MTT (3-(4,5-dimethyl-2-thiazolyl)-2,5-diphenyl-2H-tetrazolium bromide). Briefly, the day before experiment cells NIH 3T3 (mouse embryonic fibroblast cell line, ATCC CRL-1658) or HEK 293T (human embryonic kidney epithelial cell line, ATCC CRL-11268) were seeded in 96 well tissue culture plates, in RPMI 1640 culture medium supplemented with 10% fetal serum bovine, 100 units of penicillin G (sodium salt) and 100 μg of streptomycin sulfate and 2 mM L-glutamine, at a concentration that allow cells to grow exponentially during the time of the assay. Compounds to be tested were diluted in dimethylsulfoxide (DMSO) and then serially diluted in the culture medium. Compounds at different concentrations and DMSO were then added to the cells. Cells were incubated at 37°C in humidified 5% CO_2 atmosphere. After 48 hours, cell media containing DMSO (for control cells) or tested compound solution (for test cells) was removed and replaced with fresh medium containing MTT dye. After 3h of incubation the complete media was removed and the intracellular formazan crystals were solubilised and extracted with DMSO. After 15 min at room temperature the absorbance measured at 570 nm in microplate reader.

The percentage of cell viability was determined for each concentration of tested compound and the concentration of a compound reflecting a 50 % inhibition of cell viability (i.e. IC50) was determined from the concentration-response curve. This was done by applying non-linear regression procedure to the concentration response data using GraphPad PRISM software.

4.11 Chemical stability at pH 7.4

Chemical stability was determined for solutions of synthesized compounds (100 μM) in phosphate buffer (pH 7.4). Aliquots were taken in regular times and analysed by HPLC.

4.12 Stability in human plasma

Human plasma was obtained from the pooled, heparinised blood of healthy donors, and was frozen and stored at -20 °C prior to use. For the stability assay, the compounds (10 μL of a 10^{-2} M inhibitor stock solution), were incubated at 37 °C in human plasma that had been diluted to 80% (v/v) with phosphate buffer pH 7.4. Aliquots were taken in regular times, the reaction was stopped by addition of MeCN and the samples were vortexed and centrifugated for 10 min and analysed by HPLC.

4.13 Stability toward microsomal activity

Stability was assayed against Rat Pooled Liver Microsomes Male (Sprague-Dawley) 20 mg/mL from BD Gentest™. A typical incubation medium was prepared, containing 10 µL of microsomal protein, 285 µL of H_2O, 80 µL phosphate buffer (pH 7.4) and NADPH generating system [20 µL of solution A ($NADP^+$ and G6P) and 4 µL of solution B (G6PDH), both from BD Gentest™], in a 37 °C thermostatic bath. Reaction was started by addition of the test compounds (10 µL of a 10^{-3} M inhibitors stock solution). Aliquots were taken in regular times, the reaction was stopped by addition of MeCN and the samples were vortexed and centrifugated for 10 min and analysed by HPLC.

4.14 HPLC system

Merck Hitachi Pump L-2130; Column Oven L-2300; UV detector L-2400 (λ 345 nm). Column LiChroCart Purospher RP-18 (5 μm, 250-4 mm). Eluent isocratic MeOH/H_2O (80/20 v/v in 12 min runs) was used as mobile phase (1mL/min); 20 µL injection volumes.

5   References

1.   K. Imaki, T. Okada, Y. Nakayama, Y. Nagao, K. Kobayashi, Y. Sakai, T. Mohri, T. Amino, H. Nakai and M. Kawamura, *Bioorganic and Medicinal Chemistry*, 1996, **4**, 2115-2134.
2.   M. Rizzi, E. Casale, P. Ascenzi, M. Fasano, S. Aime, C. L. Rosa, M. Luisetti and M. Bolognesi, *Journal of the Chemical Society, Perkin Transactions 2*, 1993, 2253-2256.
3.   I. A. Schepetkin, A. I. Khlebnikov and M. T. Quinn, *Journal of Medicinal Chemistry*, 2007, **50**, 4928-4938.
4.   L. S. N.A. Santagati, C. Di Giacomo, L. Vanella, S. Ronsisvalle *Letters in Drug Design & Discovery*, 2007, **4**, 386-393
5.   P. E. Finke, S. K. Shah, B. M. Ashe, R. G. Ball, T. J. Blacklock, R. J. Bonney, K. A. Brause, G. O. Chandler and M. Cotton, *Journal of Medicinal Chemistry*, 1992, **35**, 3731-3744.
6.   R. J. Cvetovich, M. Chartrain, F. W. Hartner, C. Roberge, J. S. Amato and E. J. J. Grabowski, *The Journal of Organic Chemistry*, 1996, **61**, 6575-6580.
7.   A. Clemente, A. Domingos, A. P. Grancho, J. Iley, R. Moreira, J. Neres, N. Palma, A. B. Santana and E. Valente, *Bioorganic & Medicinal Chemistry Letters*, 2001, **11**, 1065-1068.
8.   J. Mulchande, R. Oliveira, M. Carrasco, L. s. Gouveia, R. C. Guedes, J. Iley and R. Moreira, *Journal of Medicinal Chemistry*, 2009, **53**, 241-253.
9.   B. Imperiali and R. H. Abeles, *Tetrahedron Letters*, 1986, **27**, 135-138.
10.   S. H. Bergeson, P. D. Edwards, R. D. Krell, A. Shaw, R. L. Stein, M. M. Stein, A. M. Strimpler, D. A. Trainor, R. A. Wildonger and D. J. Wolanin, *Abstracts of Papers of the American. Chemical Society*, 1987, **193**, 1-MEDI.
11.   K. Ohmoto, T. Yamamoto, T. Horiuchi, H. Imanishi, Y. Odagaki, K. Kawabata, T. Sekioka, Y. Hirota, S. Matsuoka, H. Nakai, M. Toda, J. C. Cheronis, L. W. Spruce, A. Gyorkos and M. Wieczorek, *Journal of Medicinal Chemistry*, 2000, **43**, 4927-4929.
12.   R. Kuang, J. B. Epp, S. Ruan, L. S. Chong, R. Venkataraman, J. Tu, S. He, T. M. Truong and W. C. Groutas, *Bioorganic and Medicinal Chemistry*, 2000, **8**, 1005-1016.
13.   M. F. Melzig, B. Loser and S. Ciesielski, *Pharmazie*, 2001, **56**, 967-970.
14.   M. Hamburger, U. Riese, H. Graf, M. F. Melzig, S. Ciesielski, D. Baumann, K. Dittmann and C. Wegner, *Journal of Agricultural and Food Chemistry*, 2002, **50**, 5533-5538.
15.   F. V. Nussbaum, D. Karthaus, S. Anlauf, M. Delbeck, D. Meibom and K. Lustig, *Bayer Pharma Aktiengesellchaft*, 2009, **Patent № 2385945**.

16.   K. R. Shreder, J. Cajica, L. Du, A. Fraser, Y. Hu, Y. Kohno, E. C. K. Lin, S. J. Liu, E. Okerberg, L. Pham, J. Wu and J. W. Kozarich, *Bioorganic & Medicinal Chemistry Letters*, 2009, **19**, 4743-4746.

17.   S. J. F. Macdonald, M. D. Dowle, L. A. Harrison, P. Shah, M. R. Johnson, G. G. A. Inglis, G. D. E. Clarke, R. A. Smith, D. Humphreys, C. R. Molloy, A. Amour, M. Dixon, G. Murkitt, R. E. Godward, T. Padfield, T. Skarzynski, O. M. P. Singh, K. A. Kumar, G. Fleetwood, S. T. Hodgson, G. W. Hardy and H. Finch, *Bioorganic & Medicinal Chemistry Letters*, 2001, **11**, 895-898.

18.   Y. Inoue, T. Omodani, R. Shiratake, H. Okazaki, A. Kuromiya, T. Kubo and F. Sato, *Bioorganic & Medicinal Chemistry*, 2009, **17**, 7477-7486.

19.   O. H. Kuromiya A, Kubo T, Imano K, Takemura T, Tsuji J, Komiya, M. , The Japanese Journal of *Pharmacology*, 2001, **85**, 559.

20.   F. V. Skiles JW, Chow G, Skoog M, *Research Communications in Chemical Pathology and Pharmacology*, 1990, **68**, 365-374.

21.   K. R. Shreder, J. Cajica, L. Du, A. Fraser, Y. Hu, Y. Kohno, E. C. K. Lin, S. J. Liu, E. Okerberg, L. Pham, J. Wu and J. W. Kozarich, *Bioorganic & Medicinal Chemistry Letters*, 2009, **19**, 4743-4746.

22.   J. W. Skiles, V. Fuchs, C. Miao, R. Sorcek, K. G. Grozinger, S. C. Mauldin, J. Vitous, P. W. Mui and S. Jacober, *Journal of Medicinal Chemistry*, 1992, **35**, 641-662.

23.   M. Gütschow, L. Kuerschner, U. Neumann, M. Pietsch, R. Löser, N. Koglin and K. Eger, *Journal of Medicinal Chemistry*, 1999, **42**, 5437-5447.

24.   H.-G. Häcker, F. Grundmann, F. Lohr, P. Ottersbach, J. Zhou, G. Schnakenburg and M. Gütschow, *Molecules*, 2009, **14**, 378-402.

25.   R. Moreira, A. B. Santana, J. Iley, J. Neres, K. T. Douglas, P. N. Horton and M. B. Hursthouse, *Journal of Medicinal Chemistry*, 2005, **48**, 4861-4870.

26.   M. Beardsell, P. S. Hinchliffe, J. M. Wood, R. C. Wilmouth, C. J. Schofield and M. I. Page, *Chemical Communications*, 2001, 497-498.

27.   W.-Y. Tsang, N. Ahmed, K. Hemming and M. I. Page, *Organic & Biomolecular Chemistry*, 2007, **5**, 3993-4000.

28.   I. Dell'Aica, L. Sartor, P. Galletti, D. Giacomini, A. Quintavalla, F. Calabrese, C. Giacometti, E. Brunetta, F. Piazza, C. Agostini and S. Garbisa, *Journal of Pharmacology and Experimental Therapeutics*, 2006, **316**, 539-546.

29.   S. J. F. Macdonald, D. J. Belton, D. M. Buckley, J. E. Spooner, M. S. Anson, L. A. Harrison, K. Mills, R. J. Upton, M. D. Dowle, R. A. Smith, C. R. Molloy and C. Risley, *Journal of Medicinal Chemistry*, 1998, **41**, 3919-3922.

30.   S. J. F. Macdonald, M. D. Dowle, L. A. Harrison, G. D. E. Clarke, G. G. A. Inglis, M. R. Johnson, P. Shah, R. A. Smith, A. Amour, G. Fleetwood, D. C. Humphreys, C. R. Molloy, M. Dixon, R. E. Godward, A. J. Wonacott, O. M. P. Singh, S. T. Hodgson and G. W. Hardy, *Journal of Medicinal Chemistry*, 2002, **45**, 3878-3890.

31.   P. D. Edwards, D. W. Andisik, A. M. Strimpler, B. Gomes and P. A. Tuthill, *Journal of Medicinal Chemistry*, 1996, **39**, 1112-1124.

32.   W. C. Groutas, N. Houserarchield, L. S. Chong, R. Venkataraman, J. B. Epp, H. Huang and J. J. McClenahan, *Journal of Medicinal Chemistry*, 1993, **36**, 3178-3181.

33.   A. Eilfeld, C. M. González Tanarro, M. Frizler, J. Sieler, B. Schulze and M. Gütschow, *Bioorganic and Medicinal Chemistry*, 2008, **16**, 8127-8135.

34.   W. C. Groutas, S. He, R. Kuang, S. Ruan, J. Tu and H.-K. Chan, *Bioorganic and Medicinal Chemistry*, 2001, **9**, 1543-1548.

35.   D. Dou, G. He, K. R. Alliston and W. C. Groutas, *Bioorganic & Medicinal Chemistry Letters*, 2011, **21**, 3177-3180.

36.   B. Löser, S. O. Kruse, M. F. Melzig and A. Nahrstedt, *Planta Med*, 2000, **66**, 751-753.

37.   K. Taori, S. Matthew, J. R. Rocca, V. J. Paul and H. Luesch, *Journal of Natural Products*, 2007, **70**, 1593-1600.

38. S. P. Gunasekera, M. W. Miller, J. C. Kwan, H. Luesch and V. J. Paul, *Journal of Natural Products*, 2009, **73**, 459-462.

39. M. T. Sisay, S. Hautmann, C. Mehner, G. M. König, J. Bajorath and M. Gütschow, *ChemMedChem*, 2009, **4**, 1425-1429.

40. L. K. Hansen P, Lepistoe M, Loenn H, Ray A, Lepisto M, Lonn H. AstraZeneca AB (ASTR), *Patent WO2007129962-A1*, 2008.

41. S. D. Lucas, E. Costa, R. C. Guedes and R. Moreira, *Medicinal Research Reviews*, 2013, **33**, E73-E101.

42. J. W. Skiles, V. Fuchs, G. Chow and M. Skoog, *Research Communications in Chemical Pathology and Pharmacology*, 1990, **68**, 365-374.

43. G. Veinberg, I. Shestakova, L. Petrulanis, N. Grigan, D. Musel, D. Zeile, I. Kanepe, I. Domrachova, I. Kalvinsh, A. Strakovs and E. Lukevics, *Bioorganic and Medicinal Chemistry Letters*, 1997, **7**, 843-846.

44. Y. Aoyama, M. Uenaka, T. Konoike, Y. Iso, Y. Nishitani, A. Kanda, N. Naya and M. Nakajima, *Bioorganic & Medicinal Chemistry Letters*, 2000, **10**, 2403-2406.

45. L. Sartor, E. Pezzato, I. Dell'Aica, R. Caniato, S. Biggin and S. Garbisa, *Biochemical Pharmacology*, 2002, **64**, 229-237.

46. L. Sartor, E. Pezzato, I. Dell'Aica, R. Caniato, S. Biggin and S. Garbisa, *Biochemical Pharmacology*, 2002, **64**, 229-237.

47. L. Wei, Z. Lai, X. Gan, K. R. Alliston, J. Zhong, J. B. Epp, J. Tu, A. B. Perera, M. V. Stipdonk and W. C. Groutas, *Archives of Biochemistry and Biophysics*, 2004, **429**, 60-70.

48. J. W. Harper, K. Hemmi and J. C. Powers, *Biochemistry-Us*, 1985, **24**, 1831-1841.

49. L. Pochet, C. Doucet, G. Dive, J. Wouters, B. Masereel, M. Reboud-Ravaux and B. Pirotte, *Bioorganic & Medicinal Chemistry*, 2000, **8**, 1489-1501.

50. S. Gérard, M. Galleni, G. Dive and J. Marchand-Brynaert, *Bioorganic and Medicinal Chemistry*, 2004, **12**, 129-138.

51. W. C. Groutas, L. S. Chong, R. Venkataraman, J. B. Epp, R. Kuang, N. Houser-Archield and J. R. Hoidal, *Bioorganic and Medicinal Chemistry*, 1995, **3**, 187-193.

52. W. C. Groutas, J. B. Epp, R. Venkataraman, R. Kuang, T. My Truong, J. J. McClenahan and O. Prakash, *Bioorganic and Medicinal Chemistry*, 1996, **4**, 1393-1400.

53. L. Pochet, C. Doucet, M. Schynts, N. Thierry, N. Boggetto, B. Pirotte, K. Y. Jiang, B. Masereel, P. de Tullio, J. Delarge and M. Reboud-Ravaux, *Journal of Medicinal Chemistry*, 1996, **39**, 2579-2585.

54. C. Doucet, L. Pochet, N. Thierry, B. Pirotte, J. Delarge and M. Reboud-Ravaux, *Journal of Medicinal Chemistry*, 1999, **42**, 4161-4171.

55. L. Crocetti, M. P. Giovannoni, I. A. Schepetkin, M. T. Quinn, A. I. Khlebnikov, A. Cilibrizzi, V. D. Piaz, A. Graziano and C. Vergelli, *Bioorganic and Medicinal Chemistry*, 2011, **19**, 4460-4472.

56. L. Wei, X. Gan, J. Zhong, K. R. Alliston and W. C. Groutas, *Bioorganic and Medicinal Chemistry*, 2003, **11**, 5149-5153.

57. C. Saturnino, M. Buonerba and A. Capasso, *Letters in Drug Design & Discovery*, 2007, **4**, 484-486.

58. B. Rennert and M. F. Melzig, *Planta Medica*, 2002, **68**, 767-769.

59. E. Colson, J. Wallach and M. Hauteville, *Biochimie*, 2005, **87**, 223-230.

60. V. M. Zakharova, O. Brede, M. Gütschow, M. A. Kuznetsov, M. Zibinsky, J. Sieler and B. Schulze, *Tetrahedron*, 2010, **66**, 379-384.

61. L. Krenn, E. Wollenweber, K. Steyrleuthner, C. Gorick and M. F. Melzig, *Fitoterapia*, 2009, **80**, 267-269.

62. G.-H. Xu, Y.-H. Kim, S.-W. Chi, S.-J. Choo, I.-J. Ryoo, J.-S. Ahn and I.-D. Yoo, *Bioorganic & Medicinal Chemistry Letters*, 2010, **20**, 513-515.

63. MOE – Molecular Operating Environment MOE.2012 Chemical Computing Group: Montreal, www.chemcomp.com).

64. GOLD 5.1, Cambridge Crystallographic Data Centre (CCDC), UK, (www.ccdc.cam.ac.uk/products/gold_suite).

65. *Bruker (2007). SAINT. Bruker AXS Inc., Madison, Wisconsin, USA.*

66. Bruker (2001). SADABS. Bruker AXS Inc., Madison, Wisconsin, USA.

67. A. Altomare, M. C. Burla, M. Camalli, G. L. Cascarano, C. Giacovazzo, A. Guagliardi, A. G. G. Moliterni, G. Polidori and R. Spagna, *Journal of Applied Crystallography*, 1999, **32**, 115-119.

68. G. M. Sheldrick, *Acta Crystallographica Section A*, 2008, **64**, 112-122.

69. L. J. Farrugia, *Journal of Applied Crystalography*, 1999, **32**, 837-838.